INVESTIGATION OF DISCRETE AND CONTINUOUS SPECRUM STATES IN TWO-CLUSTER SYSTEMS

V.S. Vasilevsky [1],* K. Kato [2],† V. Kurmangaliyeva [3],
A.D. Duisenbay [3], N. Kalzhigitov [3], and N. Takibayev [3‡]
[1] *Bogolyubov Institute for Theoretical Physics, Kiev, Ukraine*
[2] *Hokkaido University, Sapporo, Japan and*
[3] *Institute of Experimental and Theoretical Physics,*
al-Farabi Kazakh National University, Almaty, Kazakhstan

Abstract

A two-cluster microscopic model is used to study the main features of bound and resonance states in the lightest p-shell nuclei. The model correctly treats the Pauli principle and makes use of the full set of oscillator functions to expand the wave function of a two-cluster system. Interaction between clusters is determined by the superposition of semi-realistic nucleon-nucleon potentials. We present the inter-cluster wave functions in oscillator, coordinate and momentum spaces. It helps us to reveal some interesting features of the two-cluster dynamics in bound and resonance states. Phase shifts and elastic scattering cross sections are investigated in detail.

This monograph is dedicated to a deeper study of the nucleus properties and the interaction of nuclear clusters and is intended for the use of students of master and PhD courses.

PACS numbers: 21.45.+v; 28.20.Cz; 25.70.Ef; 61.12.Ex; 77.65.j

Keywords: light nuclei, clusters, bound and resonance states

*Electronic address: vsvasilevsky@gmail.com
†Electronic address: kato-iku@gd6.so-net.ne.jp
‡Electronic address: takibayev@gmail.com

I. INTRODUCTION

The analysis of astrophysical data on the abundance of light atomic nuclei in the Universe stimulates new and more detailed experimental and theoretical studies of the properties of light nuclei and reactions involving them [1–8]. Astrophysical applications of nuclear data require a more detailed and accurate determination of the cross sections of nuclear reactions in the low-energy region [9–16].

Although nuclear physics is one of the most rapidly developing fields of science in terms of theoretical and experimental research, many important and interesting issues remain still unclear in this area. Indeed, nuclear reactions involving light nuclei are largely predetermined and show the diversity of the micro and macro world, the formation and evolution of the Universe, the birth of stars and everything associated with it [9, 17, 18].

Except for the simple nucleus of a hydrogen atom, the nuclei are complex objects consisting of several interacting nucleons. Every nucleus gains the unique properties owing to peculiarities of the nuclear forces and quantum states of nucleon systems. However, the exact and detailed definition of nuclear forces associated with the properties of quark-gluon matter is still a very complicated issue. To understand the characteristic properties of every nucleus, we are compelled to use model representations of nuclei and effective nuclear interactions, relying on a number of obvious structural elements and preferential states for the corresponding nuclei. These models (see, for instance, Refs. [19–28]) can contain quasi-stationary or virtual states of nuclei, as well as their excited states located on the complex energy plane close to the real physical region of existence of the nuclei. Such models, aimed at the description of a large variety of nuclear structures and reactions, can also contain possibility of a nucleus to split or decay on two and more fragments (clusters). We recall that in nuclear physics a cluster stands for the name of sufficiently long-lived group that consist of few nucleons. Determination of a cluster-cluster interaction is important for proper interpretation of physical phenomena in nuclei [1, 29, 30].

The models proposed for the particular nucleus (and for similar mirror-nucleus) usually take into account only some of its main characteristics. Because the cluster formation strongly depends on the correlations between nucleons and properties of few-nucleon subsystems, the features of nuclear interactions are very specific and important in studies of nuclear cluster phenomena. The efficiency and reliability of cluster models have been con-

firmed by a large number of experimental data, the phenomenon of cluster radioactivity of nuclei [19, 31, 32], the compactness of α-clusters, and the formation of quasi-molecular states in nuclei and their isotopes [33–35].

At the same time, the use of cluster models greatly facilitates the theoretical calculations by reducing a many-particle problem to the effective two-body problem, provided one deals with a two-cluster system. Each cluster is considered as a stable group consisting of few nucleons interacting with other objects as a whole. The first and most rigorous formulation of a cluster model was made by J. A. Wheeler in Refs. [36, 37]. He introduced the notion "resonating group" and deduced the dynamical equations for a wave function describing the relative motion of clusters. The substantial contribution to the understanding of nuclear structures was given by Wildermuth and Tang [38]. They considered and developed the method that takes into account the cluster approximation and the Pauli principle for clusters. Several microscopic methods for solving the stationary Schrödinger equation, based on cluster model, were developed [30, 39–43], and the antisymmetrization operator was introduced to realize the Pauli principle. The main complexity of this approach was caused by calculations under the antisymmetriztion between nucleons. The development of the cluster model was brought by the microscopic methods to simplify the calculation taking into account the Pauli principle. One of these methods is the algebraic version of the resonating group method [44, 45], proposed by G. F. Filippov. The main ideas of the algebraic version [45–48] were incorporated in the calculation program "2cl_SpectrPhases.exe", which is used in the present work.

For example, we obtain that a cluster structure of a nucleus is displayed in reactions with neutrons even at low energies and with protons at energies higher than Coulomb barrier. Note that in the reactions of neutron scattering on nuclei, the low-energy region is easily achieved using available experimental setups. However, in the scattering of protons on light nuclei, the Coulomb repulsive forces obscure the effects of nuclear interactions at low energies. In such cases, the determination of the nuclear scattering cross sections based on the experimental data becomes difficult. A similar situation occurs in the reactions of the nucleous-nucleous scattering in the low-energy region. In given cases, theoretical research methods and calculations become important tools for estimating the cross sections of reactions and determining their features.

Theoretical analyses show that nuclei are not static formations that rigidly scatter neu-

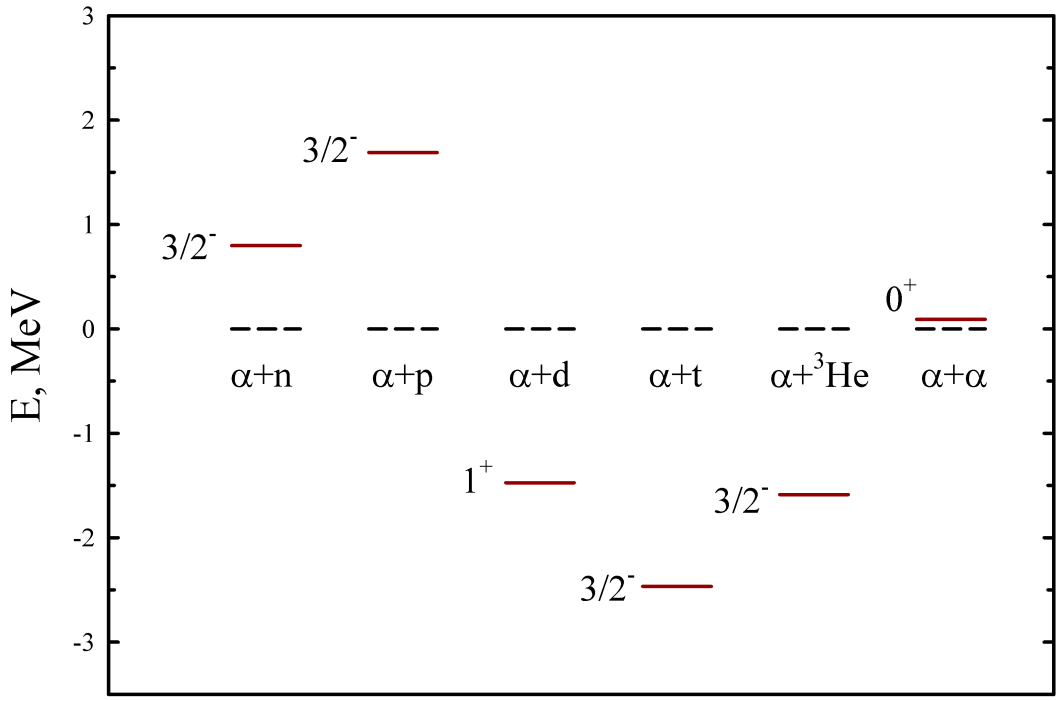

FIG. 1: Experimental energy of ground states of nuclei considered. Energy is measured with respect to the lowest two-cluster decay threshold.

trons and protons, but they are flexible structural configurations that respond to incident particles. Light nuclei are loosely bound, and they can also change their configurations (i.e. size and shape) when they interact with nucleons or other nuclei at relatively small distances between interacting nuclei. This phenomenon is called polarization of clusters [49–55].

The structure of the majority of such nuclei within the framework of the interacting clusters model gives the possibility to investigate the properties of these nuclei and their configurations [30, 38, 40]. More specifically, a nucleus as a group of dynamically interacting clusters has its own unique internal cluster structure that differs from other nuclei.

Some energy levels of light nuclei, observed in reactions experimentally, could not be occasionally explained within the simple models, such as the conventional shell model or collective models of nuclei. That is the reason why a combination of different models is often used. Among them, cluster models are important, in which it is believed that nucleons most of the time combine into various almost stable structures called clusters that interact

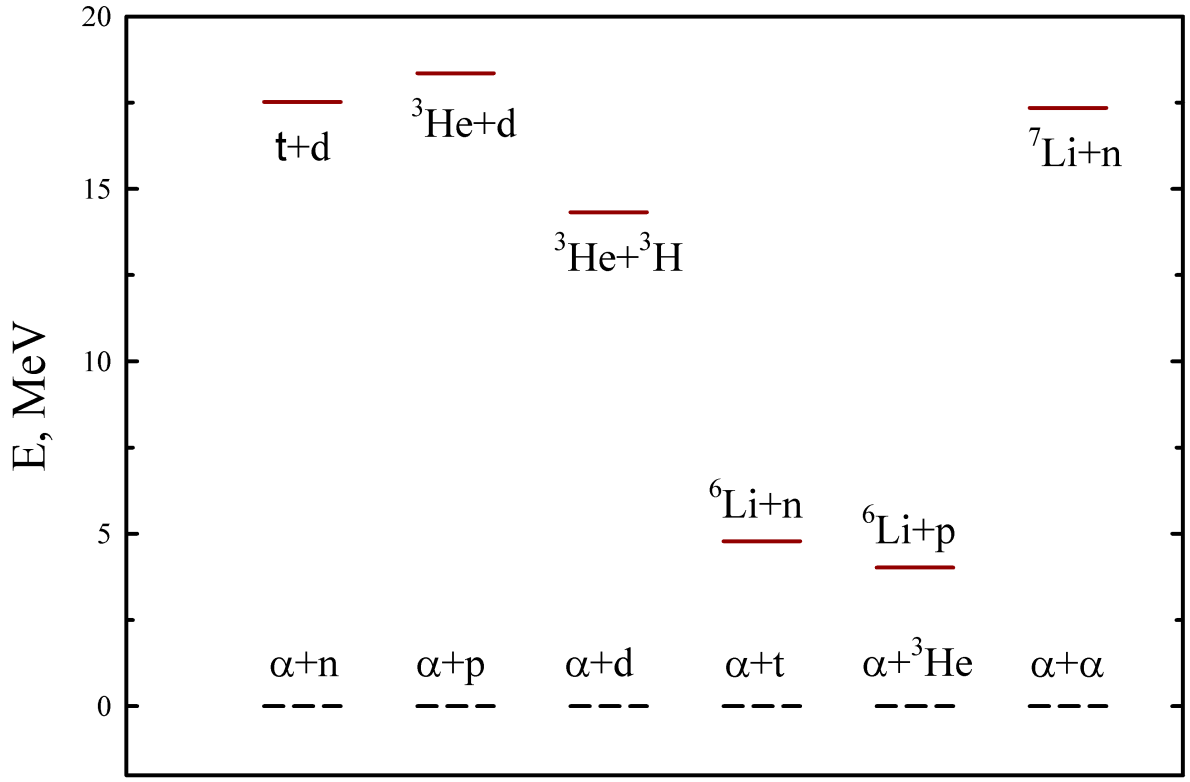

FIG. 2: Position of the second binary channel with respect to the first one. Experimental data are from Refs. [56, 57].

with each other.

The physics of clusters is historically connected with the nucleus of helium atom (α-particle) and in this choice the properties of the α particles themselves played a special role. The cluster representation of on atomic nucleus makes the calculations much simpler, by reducing the solutions to the interaction of several clusters, and neglecting their internal structure.

II. CLUSTER MODEL OF LIGHT NUCLEI

The main motivation for the model of a nucleus containing α-clusters as structural elements of nuclei is the phenomenon of the α-radioactivity and α-decay. The theory of the

α-decay of nuclei proposed by Gamow [58] implies that α-particles, i.e. α-clusters, could be formed inside the atomic nucleus before they are emitted and tunnelled through a potential barrier formed by the Coulomb and nuclear interaction potentials between an alpha particle and a residual (or daughter) nucleus.

The cluster approximation, in a number of cases, can lead to a "quasi-molecular state" in the nuclei. Such an idea comes from the fact that some nuclei with cluster structure can behave like molecules [7, 33, 34, 59]. We note that the cluster structure of light nuclei is more pronounced, although the clustering of nuclei is traced up medium-heavy nuclei, for instance, nuclei created by ^{16}O+^{40}Ca [60, 61] and ^{40}Ca+^{40}Ca [62, 63] interactions. It is clear that there are significant differences between the free α-particles and α-clusters inside the nucleus. The latter are influenced by the field created by the surrounding nucleons.

This leads to a change in the properties of the α-clusters in particular the arise polarizability, which distinguishes the α-cluster from a free α-particle not affected by the intranuclear nucleon field.

Clusters in the nucleus can exchange nucleons, break down and reassemble from the other protons and neutrons. Therefore, it is important to take into account the effective time during which an α-cluster retains its structure. If the time at which α-cluster is destroyed or transformed is significantly longer than its lifetime, then the α-cluster representation is unacceptable.

In this book, we use the resonating groups method as the most consistent cluster model for the study of the properties of ^{5}He, ^{5}Li, ^{6}Li, ^{7}Li, ^{7}Be and ^{8}Be light atomic nuclei. These nuclei are considered as a two-cluster system, where one of the clusters is an α particle, excluding the ^{8}Be nucleus consisted of two alpha-clusters. From now on we will mark a nucleus in terms of its atomic notation. In explicit form the nuclei of interest represent the following two-cluster configurations:

$$^5\mathrm{He} = \alpha + n, \quad ^5\mathrm{Li} = \alpha + p, \quad ^6\mathrm{Li} = \alpha + d, \quad ^7\mathrm{Li} = \alpha + t, \quad ^7\mathrm{Be} = \alpha +^3 \mathrm{He} \quad ^8\mathrm{Be} = \alpha + \alpha.$$

Such cluster partitioning of the investigated atomic nuclei allows us to take into account the dominant binary channel of nuclear decay into two fragments (two clusters). This channel has a minimum threshold energy among all binary channels and is responsible for most part of the observed bound and resonance states [56, 57].

Note that the ^{7}Li and ^{7}Be nuclei, consisting of seven nucleons, have a well-established two-

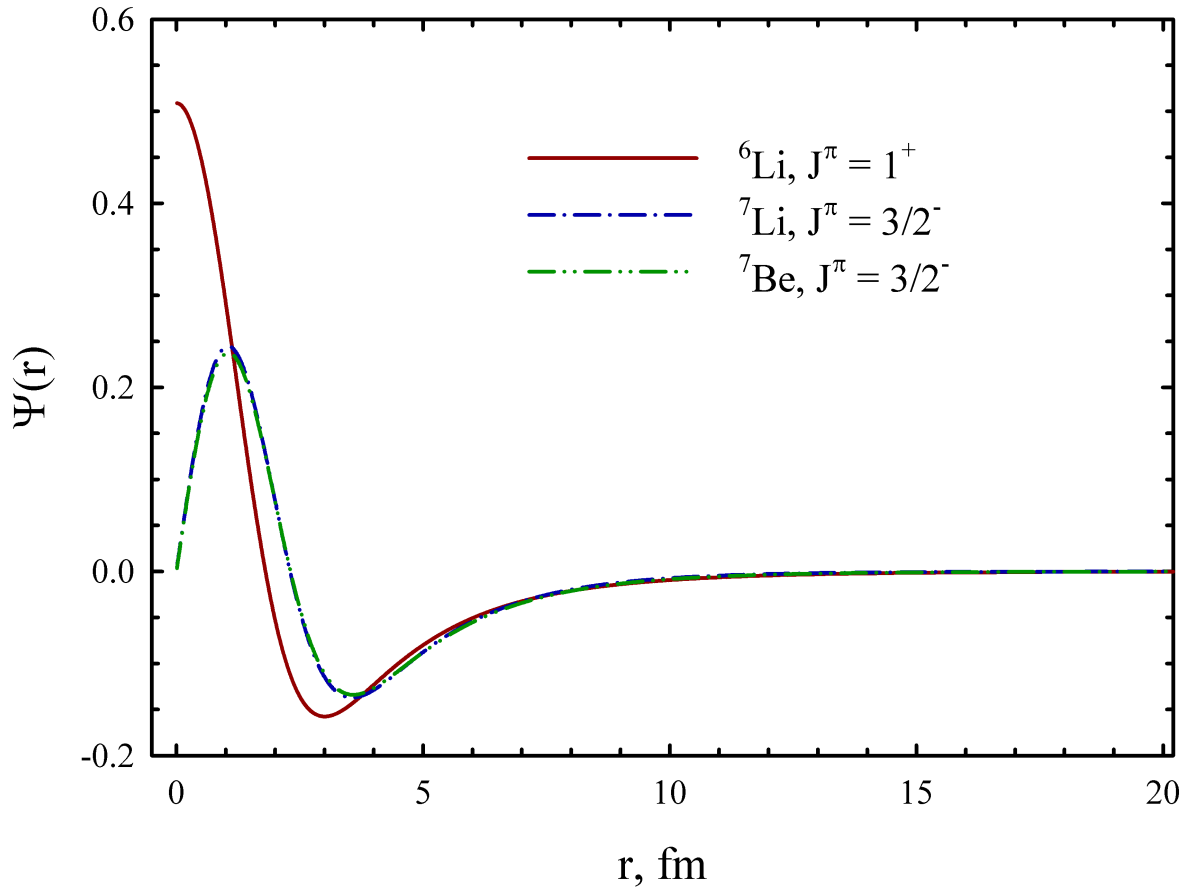

FIG. 3: Wave functions of ^{6}Li, ^{7}Li and ^{7}Be ground states as a function of the inter-cluster distance r.

cluster configuration: ^{4}He + ^{3}H and ^{4}He + ^{3}He [56, 57]. The ^{8}Li and ^{8}B nuclei are of much interest, because their two-cluster structures give a qualitative and quantitative explanation of the impossibility of existence of a stable nuclei with such atomic number. The cluster polarization gives the main contribution to the cross section of various reactions with ^{7}Li and ^{7}Be nuclei. Thus, the effects of cluster polarization were studied in the interaction of protons with ^{7}Li nuclei and neutrons with ^{7}Be nuclei [53, 64].

Indeed, the calculations show that two alpha particles cannot be bound as a long-living stable nucleus, and the alpha particle is the most compact cluster. Nevertheless, their mutual interaction turns out to be weak in the presence of strong Coulomb repulsion between the clusters [48, 57, 65]. However, the interaction of three alpha clusters gives a stable structure

- the nucleus of the carbon atom [66–70]. Thus, in the system of three clusters, the forces of nuclear attraction are stronger than Coulomb repulsive forces.

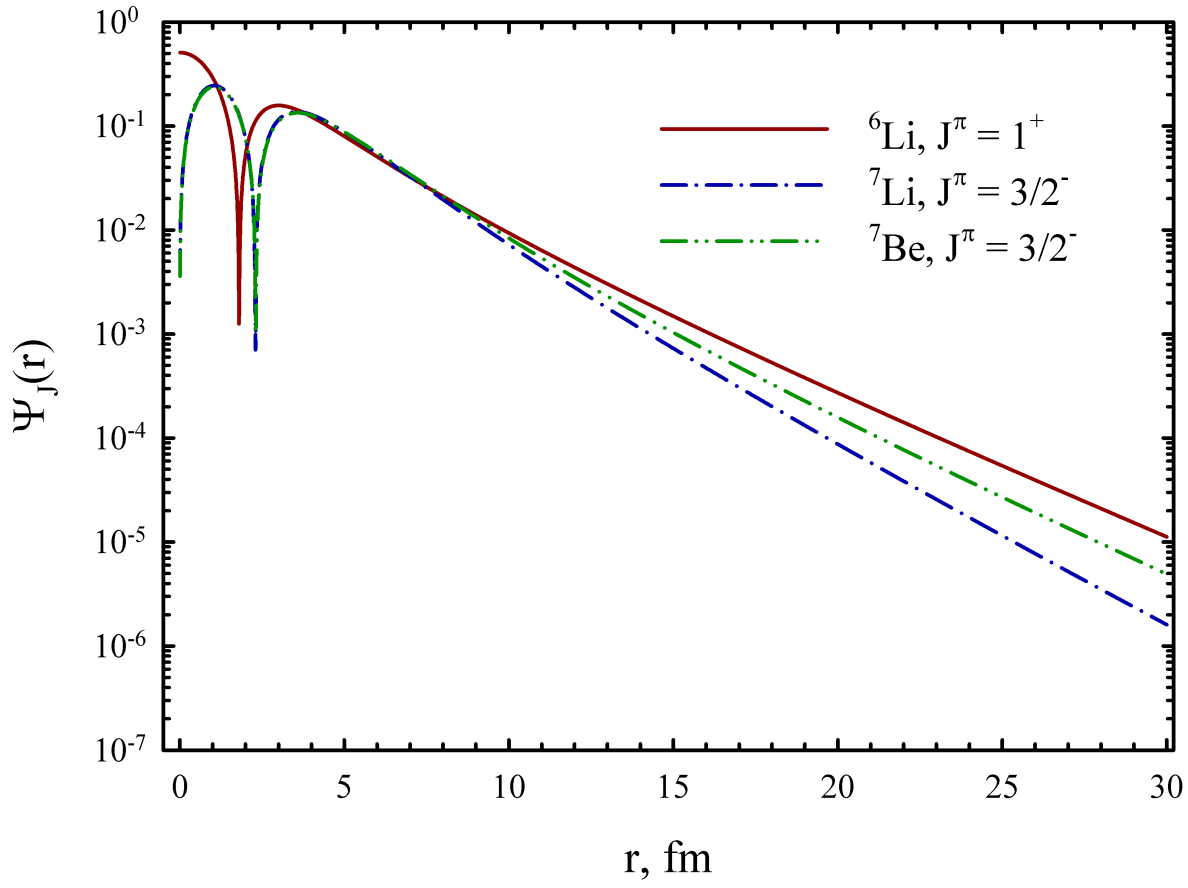

FIG. 4: Wave functions of ^{6}Li, ^{7}Li and ^{7}Be ground states as a function of the inter-cluster distance r.

The cluster structure of light nuclei is a unique dynamic construction, and cluster models describe the variety of these configurations. Note that the cluster polarization plays an important role in the formation of bound and resonance states of light, medium, and even heavy nuclei.

The present work is aimed at the investigation of a two-cluster structure the nuclei ^{5}He, ^{5}Li, ^{6}Li, ^{7}Li, ^{7}Be and ^{8}Be. We are going to study the nuclei through consideration of the interaction of alpha particles with neutrons, protons, deuterons, tritons, ^{3}He nuclei and alpha-particles. These investigations are performed within the well-known Resonating

Group Method (RGM) [38, 71], which is a self-consistent cluster model and a powerful tool for description of two- and three-cluster systems. Many interesting details of the RGM and numerous fundamental results obtained with this method are presented in a series of reviews in Refs. [59, 72, 73].

We make use of the so-called the algebraic version of the RGM (AV RGM), which was formulated in Refs. [44, 45]. The algebraic version involves a full set of oscillator functions to describe the wave functions of the inter-cluster motion. It is one of the numerous discretization schemes which are used for the numerical solution of many-cluster and many-body problems.

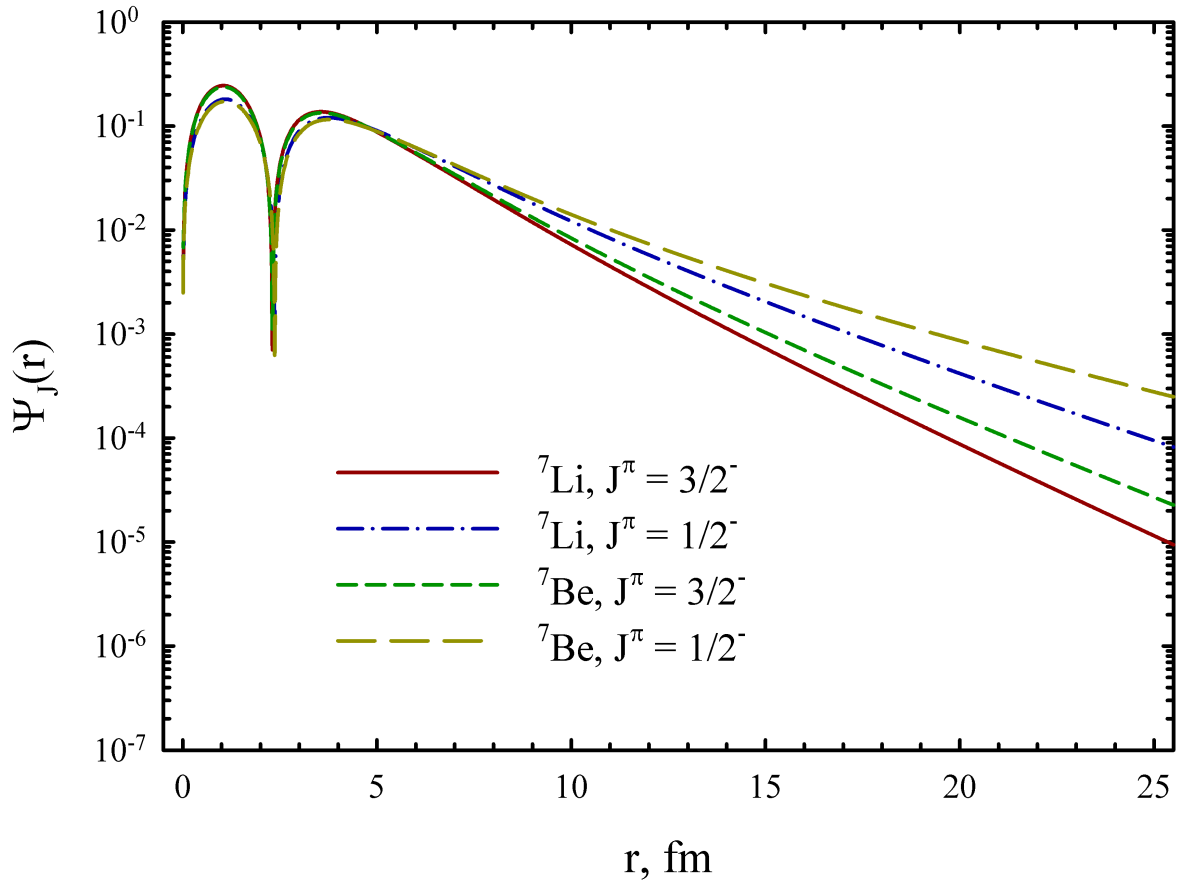

FIG. 5: Wave functions of bound state in ^{7}Li and ^{7}Be in the coordinate space.

To justify the two-cluster model, let us consider the experimental information about nuclei under consideration. Figure 1 demonstrates the importance of two body partition or

clusterization of selected nuclei. In this figure we display the experimental energy of the ground state (from Refs. [56, 57]) measured from the lowest two-cluster threshold. Nuclei ^{6}Li, ^{7}Li, ^{7}Be are presented by the bound states, while nuclei ^{5}He, ^{5}Li and ^{8}Be are presented by the lowest resonance states which are usually treated as their ground states [56, 57]. As we see, nuclei ^{6}Li, ^{7}Li, ^{7}Be can be easily split into two fragments (clusters) as their binding energy is less than 2.5 MeV, and other nuclei ^{5}He, ^{5}Li and ^{8}Be as resonance states in the two-cluster continuum. These facts unambiguously indicate the importance of a two-cluster fragmentation in the considered nuclei.

Relative position of the main two-cluster decay thresholds is displayed in Figure 2. As in the previous Figure, the energy of the second two-cluster threshold is reckoned from the first dominant threshold. Figure 2 demonstrates that for nuclei ^{5}He, ^{5}Li, ^{6}Li and ^{8}Be, the second binary channel lies far away from the first one (more than 14 MeV), and it is natural to assume that influence of the second binary channel on low energy spectrum will be negligible small. This Figure justifies the usage of a single-channel approximation for ^{5}He, ^{5}Li, ^{6}Li and ^{8}Be.

Somewhat different situation is observed in ^{7}Li and ^{7}Be, where the second binary channel is separated only by 4.78 and 4.02 MeV, respectively, from the first binary channel. In this case, we can rely on bound and continuous spectrum states below the energy of the second binary channel, where it has, as we believe, small influence on the results obtained.

Despite the long history of different versions of cluster model and the Resonating Group Method and many efforts applied, considered nuclei are still a subject for numerous theoretical investigations through different theoretical methods. These Methods include the traditional Resonating Group Method and its modifications such as the Antisymmetric Molecular Dynamics [74] or Fermionic Molecular Dynamics [75, 76], and novel methods such as *ab initio* No-Core Shell Model [67, 77–79] or Effective Field Theory [65, 69]. There are many interesting features of these nuclei, which have to be thoroughly considered and systemized, especially in their continuous spectrum. It is well-known that with simple models one can easily obtain results of general character, or establish some interesting relationships between different physical quantities, which are valid in more complicated and advanced models.

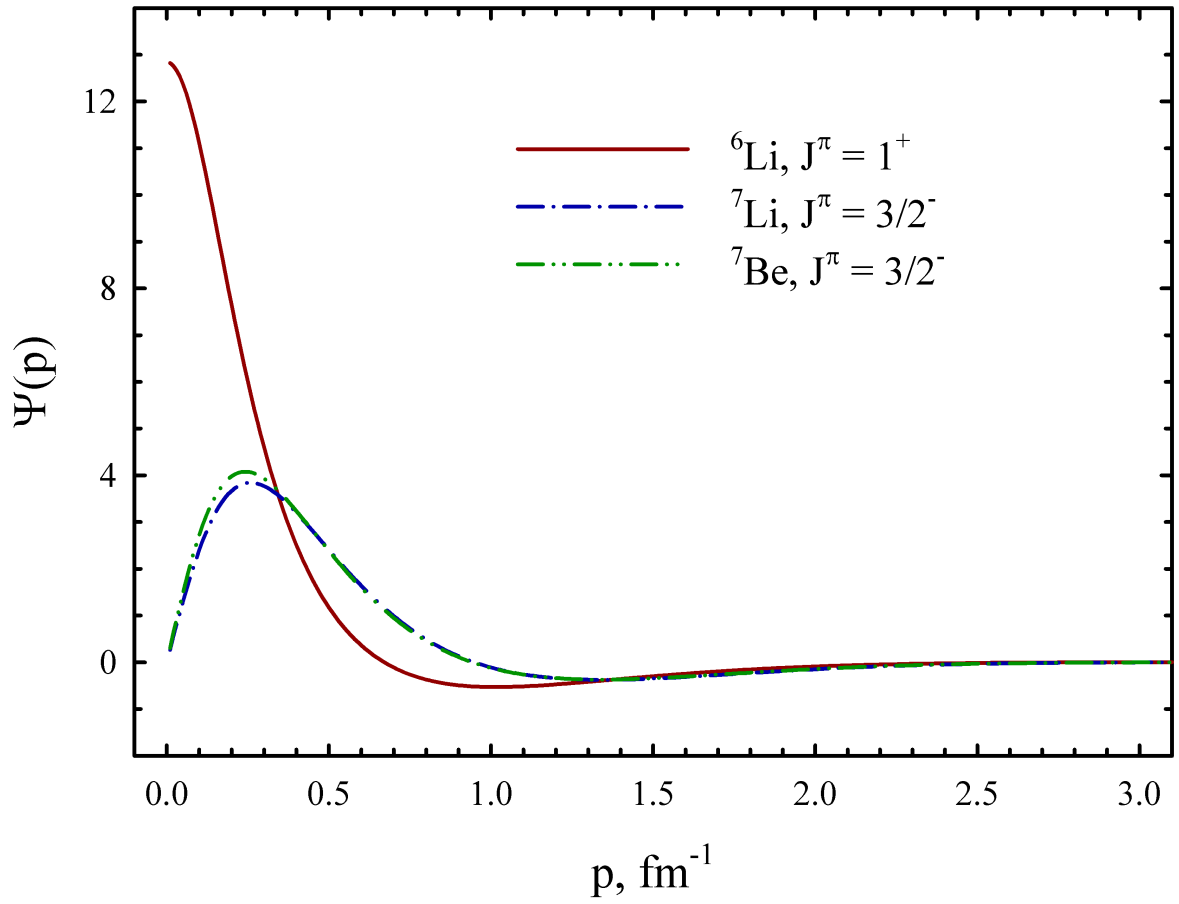

FIG. 6: Wave functions of the ^{6}Li, ^{7}Li and ^{7}Be ground states in the momentum space.

III. MODEL FORMULATION

In this section, we briefly present some important details of the Algebraic or Matrix version of the Resonating Group Method. A Hamiltonian and the form of a wave function of a many-particle system are two main ingredients of any microscopic model. Thus, we start formulation of our model with a microscopic Hamiltonian.

Hamiltonian for a nucleus consisting of A nucleons is represented by two terms the kinetic energy and potential energy:

$$\hat{H} = \hat{T} + \hat{V}, \tag{1}$$

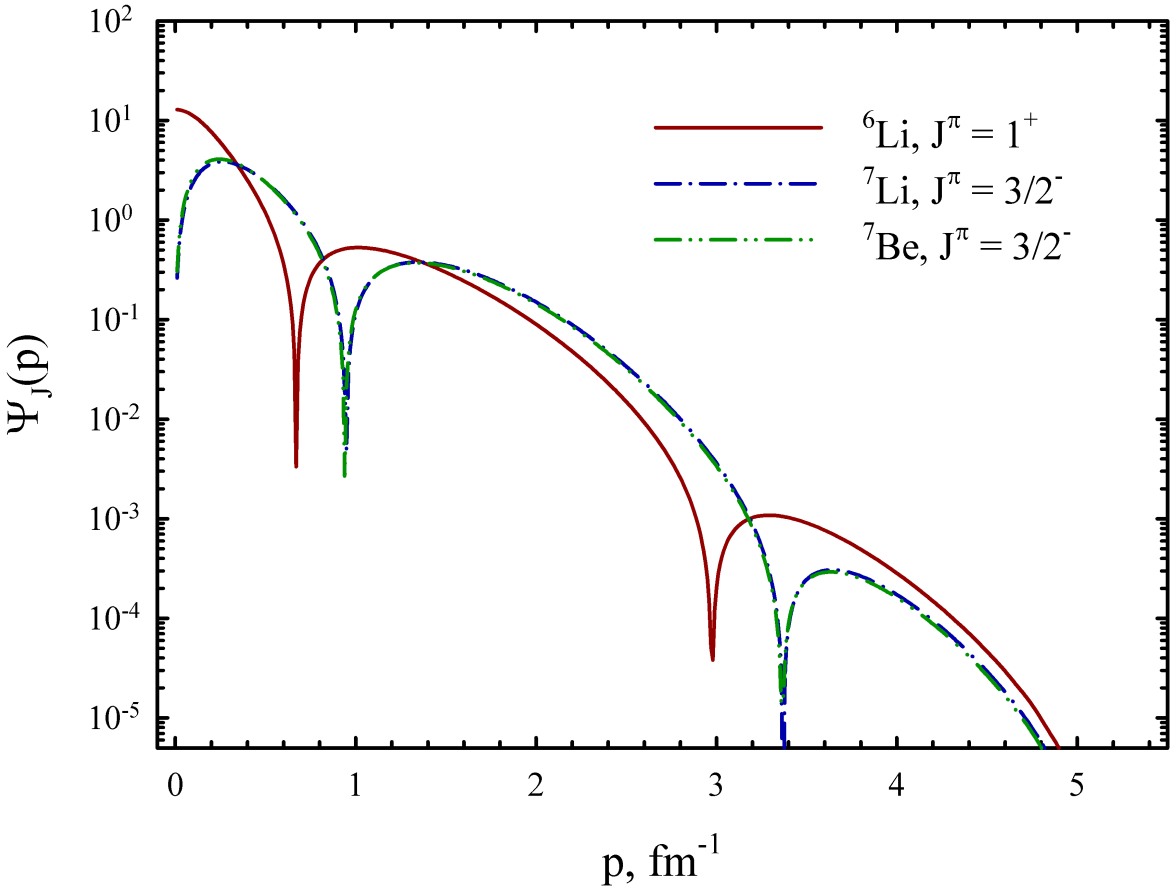

FIG. 7: Wave functions of the ground states in ^{6}Li, ^{7}Li and ^{7}Be as a function of the relative momentum p.

where the kinetic energy is determined in the center of mass system coordinates

$$\hat{T} = -\frac{\hbar^2}{2m}\sum_{i=1}^{A}\Delta_i + \frac{\hbar^2}{2m}\Delta_R. \tag{2}$$

Within our model, the potential energy $\hat{V}$ is determined by a semi-realistic nucleon-nucleon interaction. We split the operator $\hat{V}$ on three components

$$\hat{V} = \sum_{j>i=1}^{A}\hat{V}^{(cn)}(ij) + \sum_{j>i=1}^{A}\hat{V}^{(so)}(ij) + \sum_{j>i=1}^{A}\hat{V}^{(C)}(ij). \tag{3}$$

They represent the central nucleon-nucleon interaction: $\hat{V}^{(cn)}(ij)$, the spin-orbital interaction: $\hat{V}^{(so)}(ij)$ and the Coulomb forces: $\hat{V}^{(C)}(ij)$. The central nucleon-nucleon interaction

is

$$\hat{V}^{(cn)}(ij) = \sum_{S=0,1} \sum_{T=0,1} V^{(cn)}_{2S+1,2T+1}(ij) \hat{P}_S(ij) \hat{P}_T(ij), \tag{4}$$

where S and T are the spin and isospin of a two-nucleon system, respectively. The operators $\hat{P}_S(ij)$ and $\hat{P}_T(ij)$ project a two-nucleon state onto the state with definite values of spin S ($S = 0, 1$) and isospin T ($T = 0, 1$).

An alternative form of a nucleon-nucleon interaction also involves four components: Wigner, Majorana, Bartlett and Heisenberg interactions. The spin-orbital interaction $\hat{V}^{(so)}(ij)$ takes place only with the two-nucleon spin $S = 1$ and thus consists of two terms:

$$\hat{V}^{(so)}(ij) = \sum_{T=0,1} V^{(so)}_{S,2T+1}(ij) \hat{P}_{S=1}(ij) \hat{P}_T(ij) (\hat{l}_{ij} \hat{s}_{ij}), \tag{5}$$

where $\hat{l}_{ij}$ is the orbital momentum operator and $\hat{s}_{ij}$ is two-nucleon spin operator. The Coulomb interaction is

$$\hat{V}^{(C)}(ij) = e^2 / r_{ij},$$

where $r_{ij} = |\mathbf{r}_i - \mathbf{r}_j|$ is a distance between interacting nucleons.

Radial part of nucleon-nucleon potentials, which we are going to use, is expressed as a combination of Gaussians

$$V^{(\nu)}_{2S+1,2T+1}(j) = \sum_{i=1}^{N_G} V^{(\nu,i)}_{2S+1,2T+1} \exp\left\{-(r_{ij}/a^{\nu,i}_{2S+1,2T+1})^2\right\}, \tag{6}$$

where constants $V^{(\nu,i)}_{2S+1,2T+1}$ and $a^{\nu,i}_{2S+1,2T+1}$ determine the intensity and radius of the ν component of a nucleon-nucleon interaction ($\nu = cn$ or $\nu = so$), respectively.

The second ingredient of our model (a wave function) indicates which part of the total Hilbert space is taken into account and is represented in the form

$$\Psi_{EJ} = \hat{A} \left\{ [\Phi_1(A_1, s_1) \Phi_2(A_2, s_2)]_S \, \psi^J_{ELS}(q) Y_L(\hat{\mathbf{q}}) \right\}_J, \tag{7}$$

where $\hat{A}$ is the antisymmetrization operator, $\Phi_1(A_1, s_1)$ and $\Phi_2(A_2, s_2)$ are the translationary invariant and antisymmetric functions describing internal structure of the first and second clusters, respectively; s_1 and s_2 are spins of clusters. A wave function $\psi^J_{ELS}(q)$ represents radial motion two clusters, while the spherical harmonic $Y_L(\hat{\mathbf{q}})$ represents rotating motion

of clusters. The Jacobi vector $\mathbf{q} = q \cdot \hat{\mathbf{q}}$ ($\hat{\mathbf{q}}$ is a unit vector) is proportional to the distance r between interacting clusters

$$\mathbf{q} = \mathbf{r}\sqrt{\frac{A_1 \cdot A_2}{A_1 + A_2}} = \sqrt{\frac{A_1 \cdot A_2}{A_1 + A_2}} \left[\frac{1}{A_1} \sum_{i \in A_1} \mathbf{r}_i - \frac{1}{A_2} \sum_{j \in A_2} \mathbf{r}_j \right], \tag{8}$$

where $\mathbf{r}_1$, $\mathbf{r}_2$, ..., $\mathbf{r}_A$ are positions of individual nucleons in the coordinate space.

As one can see from Eq. (7), two-cluster systems will be investigated in the LS coupling scheme. In this scheme the total spin S of a system is a vector sum of individual spins of clusters $\mathbf{S} = \mathbf{s}_1 + \mathbf{s}_2$, and the total angular momentum J is a vector sum of the total orbital momentum L and total spin S: $\mathbf{J} = \mathbf{L} + \mathbf{S}$. As we deals with two s-clusters, then the total orbital momentum L coincides with the orbital momentum of the relative motion of clusters. Moreover, within the present model both total orbital momentum L and total spin S are good quantum numbers.

The main assumption of the RGM is that wave functions $\Phi_1(A_1; s_1)$ and $\Phi_2(A_2; s_2)$ are known and fixed, while the inter-cluster function $\psi^J_{ELS}(q)$ has to be obtained by solving the dynamic equations. In the standard version of the RGM, one has to solve the integro-differential equation. The integral or nonlocal part of the equation appears due to the antisymmetrization operator or, in other words, due to the Pauli principle. In the algebraic version of RGM, the dynamic equations transforms in to a set of linear algebraic equations. This is achieved by using a full set of the radial part of oscillator functions $\Phi_{nL}(q, b)$. By expanding the inter-cluster function $\psi^J_{ELS}(q)$ over oscillator functions

$$\psi^J_{ELS}(q) = \sum_{n=0}^{\infty} C_{nL;SJ}\ \Phi_{nL}(q, b) \tag{9}$$

or the total two-cluster function Ψ_{EJ} over cluster oscillator functions $|nL; SJ\rangle$

$$\Psi_{EJ} = \sum_{n=0}^{\infty} C_{nL;SJ}\, |nL; SJ\rangle\,, \tag{10}$$

we arrive to a system of linear algebraic equations

$$\sum_{\widetilde{n}=0}^{\infty} \left\{ \left\langle nL|\widehat{H}|\widetilde{n}L \right\rangle - E\, \langle nL|\widetilde{n}L\rangle \right\} C_{\widetilde{n}L;SJ} = 0, \tag{11}$$

where $\left\langle nL|\widehat{H}|\widetilde{n}L \right\rangle$ is a matrix elements of a microscopic hamiltonian between oscillator functions, and $\langle nL|\widetilde{n}L\rangle$ is a matrix element of the antisymmetrization operator or norm

kernel. For two cluster systems under consideration, matrix elements $\langle nL|\widetilde{n}L\rangle$ have a very simple form

$$\langle nL|\widetilde{n}L\rangle \ = \lambda_n \delta_{n,\widetilde{n}}. \tag{12}$$

The cluster oscillator function $|nL;SJ\rangle$ is determined as

$$|nL;SJ\rangle = \widehat{A}\left\{\left[\Phi_1(A_1,s_1)\Phi_2(A_2,s_2)\right]_S \Phi_{nL}(q,b)Y_L(\hat{\mathbf{q}})\right\}_J, \tag{13}$$

and here is the explicit form of the oscillator functions ($\rho = q/b$)

$$\Phi_{nL}(q,b) = (-1)^n N_{nL} b^{-3/2} \rho^L \exp\{-\rho^2/2\} L_n^{L+1/2}(\rho^2). \tag{14}$$

As we interested in the inter-cluster wave function in the momentum space $\psi^J_{ELS}(p)$, we present also oscillator functions in momentum space ($\rho = pb$)

$$\Phi_{nL}(p,b) = N_{nL} b^{3/2} \rho^L \exp\{-\rho^2/2\} L_n^{L+1/2}(\rho^2), \tag{15}$$

where

$$N_{nL} = \sqrt{\frac{2\Gamma(n+1)}{\Gamma(n+L+3/2)}}, \tag{16}$$

and $L_n^\alpha(z)$ is the generalized Laguerre polynomial [80].

The system of equations (11) is totally equivalent to the Schrödinger equation

$$\left(\hat{H} - E\right)\Psi_{EL} = 0$$

for the wave function (7). By solving the set of equations (11), one obtains the energy and a wave function of bound states, or a wave function and the scattering S-matrix for continuous spectrum states. If in Eq. (11) we restrict ourselves with a finite number (we denote it N) of oscillator function ($n = 0,\ 1,\ \ldots,\ N-1$), we encounter the generalized eigenvalue problem for $N \times N$ matrices. By solving this problem, we obtain energy and wave functions of bound and pseudo-bound states. The physical meaning of the pseudo-bound state is thorough discussed in Ref. [81]. To solve the system of equations (7) for a scattering state, one has to incorporate in these equations proper boundary conditions. We will not dwell on adopting of equations (7) to the continuous spectrum states as this matter has been numerously discussed in literature (see, for instance, [44, 45, 82, 83], [47]).

We will not also dwell on calculating of matrix elements of the kinetic and potential energy operators, as their explicitly form and reliable methods of their calculations can be found in [47].

It is important to note that wave function Ψ_{EL} for bound and pseudo-bound states is traditionally normalized to unit

$$\langle \Psi_{EL} | \Psi_{EL} \rangle = \sum_{n=0}^{\infty} |C^J_{nLS}|^2 = 1, \tag{17}$$

that corresponding inter-cluster function is normalized as $\left\langle \psi^J_{ELS} | \psi^J_{ELS} \right\rangle = S_{LJ}$. In oscillator representation S_{LJ} can be represented as

$$S_{LJ} = \sum_{n=0}^{\infty} |C^J_{nLS}|^2 / \lambda_n. \tag{18}$$

The quantity S_{LJ} proportional to the spectroscopic factor SF_{LJ} (see definition, for instance, in Refs. [84], [85] and [86], Chapter 9)), which play an important role in the theory of nuclear reactions when the Pauli principle is treated approximately [85]. The factor SF_{LJ} is used to determine amount of a certain (definite) clusterization in a wave function of the compound system. It is obvious from the definition of the spectroscopic factor (17) and (18), that it can be determined for bound state only, when norms of wave functions Ψ_{EL} and ψ^J_{ELS} are finite. A more detailed description of the calculation technique can be found in the Appendix.

IV. INPUT PARAMETERS OF CALCULATIONS

To perform all necessary calculations, we have to select the only one free parameter of the model - the oscillator length b. We chose the oscillator length to minimize energy of the two-cluster threshold. Such a choice provides an optimal description of internal structure of alpha particle in nuclei ^{5}He, ^{5}Li and ^{8}Be. For nuclei ^{6}Li, ^{7}Li and ^{7}Be the optimal value of the oscillator length allows us to describe in average the internal structure of pair of clusters: α and d, α and t, α and ^{3}He, respectively. Calculations of discrete and continuous spectrum of two-cluster systems are carried out with the modified Hasegawa-Nagata potential (MHNP) [87, 88], which contains central and spin-orbital components, and Coulomb forces between protons are also involved. The MHNP was specially constructed for investigating cluster

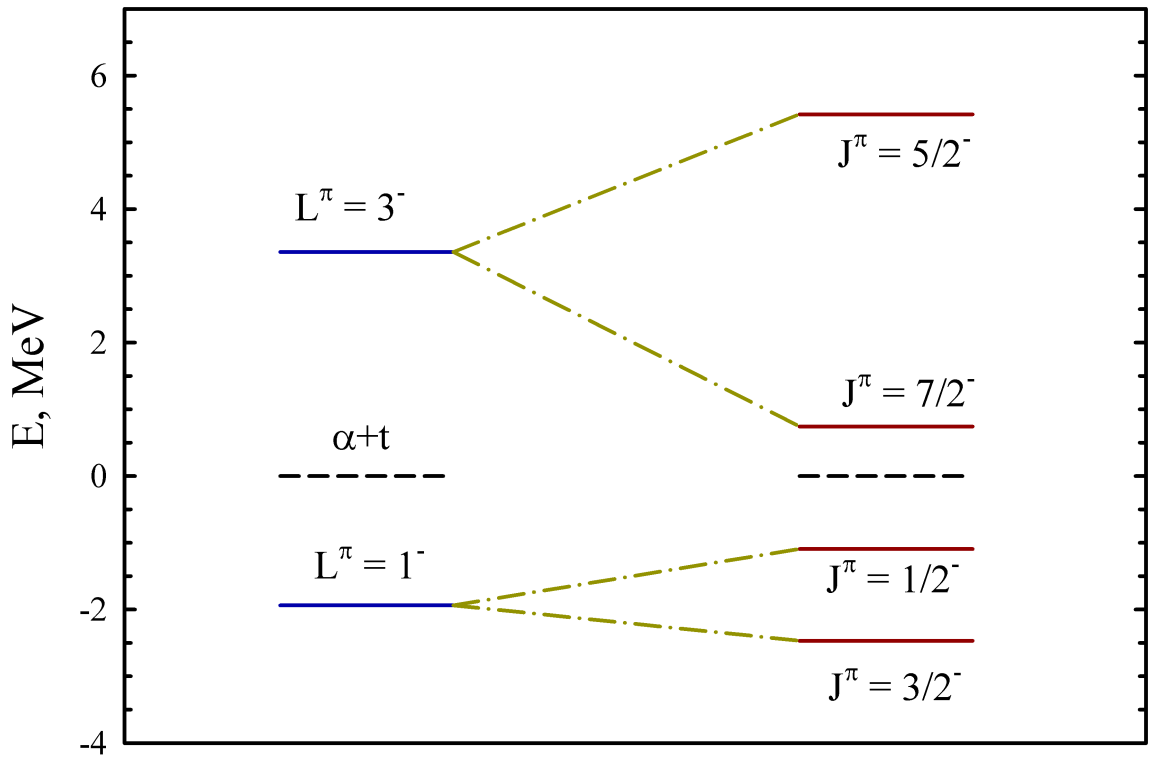

FIG. 8: Spectrum of bound and resonance states in ^{7}Li obtained with (right-hand side) and without (left-hand side) the spin-orbital interaction.

structure of light nuclei. It has been very often used to study nuclear structure and nuclear reactions within different variants of the Resonating Group Method.

To be more consistent with the experimental situation, we slightly change the Majorana parameter m of the Hasegawa-Nagata potential to reproduce position of the ground states of nuclei ^{6}Li, ^{7}Li and ^{7}Be and lowest resonance states in ^{5}He, ^{5}Li and ^{8}Be with respect to the dominant two-cluster threshold. The optimal values of input parameters (the oscillator length b and the Majorana parameter m) are listed in Table I.

Actually, we indicate modification of the Majorana parameter m with respect to original value $m_0 = 0.4057$. It is done in order to demonstrate that modifications are rather small.

It is turn out that the spin-orbital components of the MHNP are too strong which leads to unphysical results, such as too strongly bound states or to appearance of new bound states,

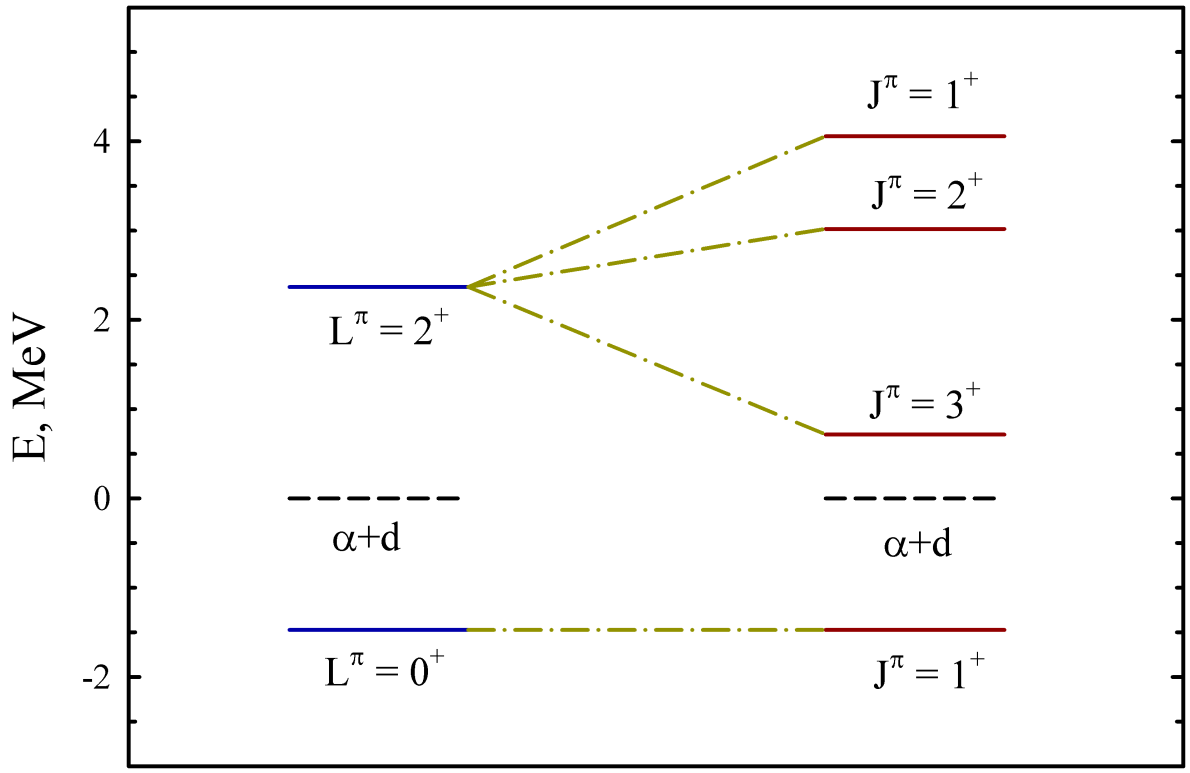

FIG. 9: Effects of the spin-orbital interaction on the spectrum of bound and resonance states in ^{6}Li.

which are not observed experimentally. To avoid such problems we introduce a common factor f_{LS} for the spin-orbital forces and used it as a variational parameter.

One can see in Table I, that strong modification of the intensity of the spin-orbital forces is need to place the $3/2^-$ resonance state in ^{5}He and ^{5}Li, and also to place the very narrow 3^+ resonance state in ^{6}Li. Resonance structure of all nuclei will be considered in details in the following sections. To see more explicitly effects of the Coulomb forces on spectrum of bound and resonance states, we use the same input parameters for mirror nuclei ^{5}He and ^{5}Li, ^{7}Li and ^{7}Be.

In Table II we collect the main parameters of the bound states in ^{6}Li, ^{7}Li and ^{7}Be. We display energy of the bound states E, root-mean-square (rms) radii proton (R_p), neutron (R_n) and mass (R_m), quadrupole moment Q and spectroscopic factor SF_{LJ}. Theoretical

TABLE I: Input parameters of the present calculations.

Nucleus	b, fm	Δm	f_{LS}
^{5}He, ^{5}Li	1.317	0.000	0.50
^{6}Li	1.357	-0.0009	0.348
^{7}Li, ^{7}Be	1.362	0.0002	1.000
^{8}Be	1.317	-0.0078	-

TABLE II: Properties of bound states in ^{6}Li, ^{7}Li and ^{7}Be, determined within the two-cluster model and with MHNP.

Nucleus	J^π	E, MeV	R_p, fm	R_n, fm	R_m, fm	Q e·fm^2	SF_{LJ}
^{6}Li	0^+	-1.473	2.36	2.36	2.36	-	0.93
^{7}Li	$3/2^-$	-2.467	2.23	2.33	2.29	-3.04	0.863
^{7}Li	$1/2^-$	-1.093	2.46	2.57	2.52	-	0.879
^{7}Be	$3/2^-$	-1.588	2.38	2.27	2.33	-5.14	0.865
^{7}Be	$1/2^-$	-0.310	2.68	2.57	2.64	-	0.885

results, obtained within our two-cluster model, are compared with the available experimental data in Table III. Experimental data are taken from Refs. [56, 57]. It is deduced from Table III that our model provides a satisfactory description of ground state properties of ^{6}Li, ^{7}Li and ^{7}Be.

TABLE III: Experimental data for bound states in ^{6}Li, ^{7}Li and ^{7}Be.

Nucleus	J^π	E, MeV	R_p, fm	R_m, fm	Q e·fm^2
^{6}Li	0^+	-1.473	2.57± 0.10	-	-
^{7}Li	$3/2^-$	-2.467	2.43± 0.02	2.78± 0.03	-3.83± 0.03
^{7}Be	$3/2^-$	-1.588	2.53± 0.03	-	-

In Table IV we compare our results for bound states with results of more advanced cluster models (namely, the microscopic three-cluster models). In this Table, we display the energy of bound states (in MeV), the proton (R_p), neutron (R_n) and mass (R_m) root-mean-square

radii (in fm) and also the quadrupole moment (in $e{\cdot}fm^2$). In Refs. [50, 52, 89] a three-cluster model (which is referred to as the AM GOB) was used to study bound states properties of ^{7}Li and ^{7}Be, and different nuclear reactions as well. We also included results of T.Kajino et al, which were obtained within the other version of the Resonating Group Method [90, 91], and results of K. Varga et al [92], who applied the Stochastic Variational Method. Calculations of ^{6}Li were performed within the Generator Coordinate Method (GCM) by Cst and Lovas [93] and within a microscopic three-cluster model by Arai et al [94].

TABLE IV: Properties of bound states in ^6Li,^{7}Li, ^{7}Be determined within different models.

Method	Nucleus	J^π	E, MeV	R_p	R_n	R_m	Q	SF_{LJ}
AV RGM	^{6}Li	1^-	-1.473	2.36	2.36	2.36	-	0.93
Arai [94]		1^-	-1.441	2.44	2.44	2.44		
GCM [93]			-1.534	2.763		2.643		0.93
AV RGM	^{7}Li	$3/2^-$	-2.467	2.23	2.33	2.29	-3.04	0.863
		$1/2^-$	-1.093	2.46	2.57	2.52	-	0.879
AM GOB		$3/2^-$	-2.640	2.23	2.34	2.41	-4.05	0.994
Kajino [90, 91]		$3/2^-$	-2.473	2.55	2.57		-4.41	0.879
Varga [92]		$3/2^-$		2.28	2.38	2.34		
AM RGM	^{7}Be	$3/2^-$	-1.588	2.38	2.27	2.33	-5.14	0.865
		$1/2^-$	-0.310	2.69	2.57	2.64	-	0.885
AM GOB		$3/2^-$	-1.702	2.46	2.26	2.38	-6.25	0.986
Kajino [90, 91]		$3/2^-$	-1.548	2.74	2.50		-7.35	
Varga [92]		$3/2^-$		2.41	2.31	2.36	-6.11	

Results presented in Table IV, show that the simple two-cluster model, which is used in the present paper, quite correctly reproduces main properties of the bound states in ^{6}Li, ^{7}Li and ^{7}Be, and is comparable and consistent with more advanced microscopic models. It means that the present model takes into account main properties of the nuclei considered and it also indicates that two-cluster channels selected plays a very important role in formation of bound

states and, as we will see later, of continuous spectrum states as well. The spectroscopic factors SF_{LJ}, as was mentioned early, reveals effects of the Pauli principle on wave functions of inter-cluster motion. Deviation of the spectroscopic factor from unity indicates how strong is effect of the Pauli principle. The most strong effect is observed for the ground state of ^{7}Li nucleus, where $SF_{LJ} = 0.863$ and most weak effect is observed in the ground state of ^{6}Li: $SF_{LJ} = 0.930$. Note that approximately such a value of the spectroscopic factor was obtained in other microscopical calculations, see Ref. [95] and citations in it.

Let us consider wave functions of bound states. In Figures 3, 4 and 5 we display wave functions of the ground states in ^{6}Li, ^{7}Li and ^{7}Be and wave functions of bound states in ^{7}Li and ^{7}Be. As we can see in Figure 3, the wave function of ground states of two-cluster systems has a node at small inter-cluster distances.

Usually in a simple quantum two-body systems, wave function of the ground state has no nodes. However, there are one or more nodes in two-cluster systems. They appear due to the Pauli principle. This property of two- and many-cluster wave functions allowed S. Saito to suggest a more simple version of the RGM, which is now called the Orthogonality Condition Model (OCM) and which takes into account the Pauli principle approximately [96, 97].

Figures 4 and 5 are presented in logarithmic scale in order to observe main differences in behavior of the wave functions. We can see that the deeper is a bound state, the faster decrease its wave function. Figures 4 and 5 demonstrate very important feature of the present calculations. Wave functions of bound states have an exponential tale, as one should expect, despite we use oscillator functions, which have Gaussian tale. Thus, our model (namely, the algebraic version of the RGM) correctly describes the energies of bound states and their wave functions as well.

To get more information about bound states in ^{6}Li, ^{7}Li and ^{7}Be, we present their wave functions in the momentum space in Figure 6 and 7. As we can see wave functions of the ^{7}Li and ^{7}Be ground states are almost indistinguishable especially in logarithmic scale.

Wave functions of the bound states are decreasing faster in momentum space than in coordinate space. It is important to recall that wave functions of bound states have very definite asymptotic form in the coordinate space, while wave functions of these states in the momentum space have no definite asymptotic form.

The spin-orbital components of NN-interaction take part in formation of bound and

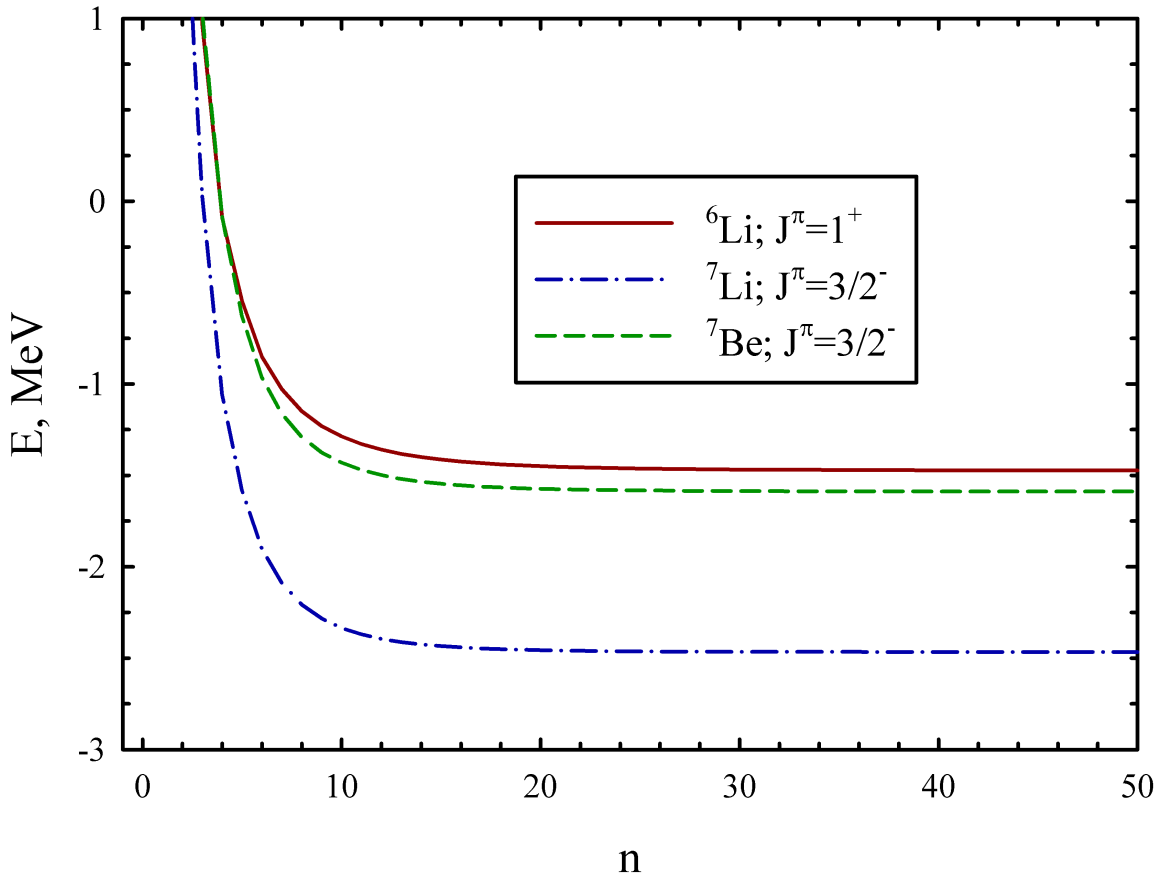

FIG. 10: The energy of the ground states in ^{6}Li, ^{7}Li and ^{7}Be as a function of a number n of oscillator functions.

resonance states in odd and odd-odd nuclei. In our case, spectrum of ^{5}He, ^{5}Li, ^{6}Li, ^{7}Li, ^{7}Be nuclei is obtained with the spin-orbital forces. Figure 8 demonstrates effects of the spin-orbital forces on energy of bound and resonance states in ^{7}Li. In left-hand side of the Figure 8, we show the spectrum of ^{7}Li calculated without the spin-orbital forces, while the right-hand side of Figure 8 display the ^{7}Li spectrum obtained with the spin-orbital forces.

When the spin-orbital forces are disregarded, the total orbital momentum L become the integral of motion. One can see that, the spin-orbital forces play an important role in formation of bound and resonance state in ^{7}Li. Effects of the spin-orbital interaction on spectrum of ^{6}Li are shown in Figure 9. Similar picture was also observed in nuclei ^{5}He, ^{5}Li and ^{7}Be.

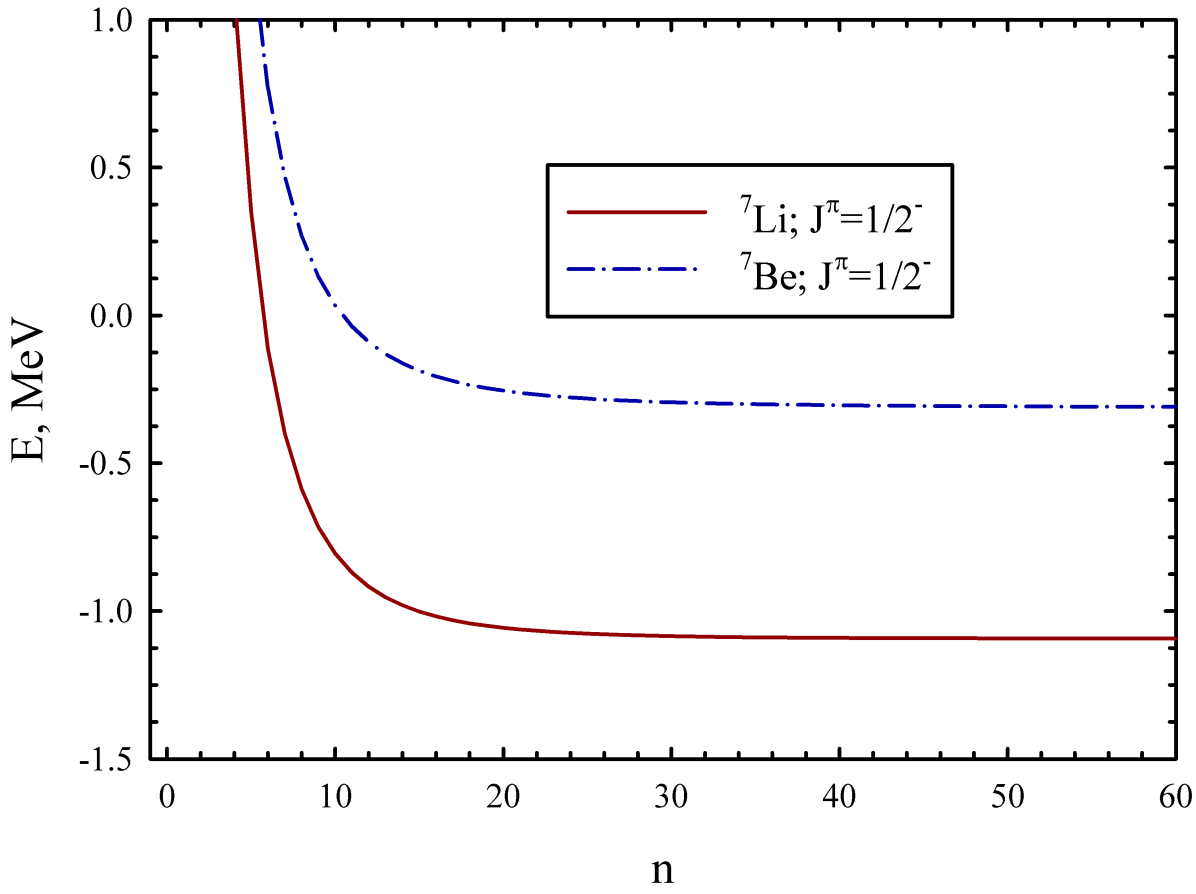

FIG. 11: Convergence of energy of the $1/2^-$ excited states in ^{7}Li and ^{7}Be.

V. CONVERGENCE

As it was pointed above, we make use the oscillator basis functions to expand wave functions of bound and continuous spectrum states of two-cluster systems. The first question, which may appear in this respect, whether our basis is large enough to obtain stable and reliable results. To answer this question we present Figure 10 where we display how energy of the ground state in ^{6}Li, ^{7}Li and ^{7}Be depends on number n of oscillator functions involved in calculations. Note that nucleus ^{7}Li is more deeply bound than the other nuclei comparing to ^{6}Li and ^{7}Be. As one can see, five oscillator functions are necessary to bound these nuclei.

To obtain the convergent energy, we need to use $n = 30 - 35$ functions. With such a number of functions, we obtain energy of the ground states with very high precision.

There are excited $1/2^-$ states in ^{7}Li and ^{7}Be. They are loosely bound states. However, as we can see in Figure 11, to provide convergent results we also need not very huge set of oscillator functions. Indeed, in our calculations, energy of the $1/2^-$ excited state of ^{7}Be is small $E = -0.31$ MeV, but it can be obtained with less than 60 functions.

Later we will discuss convergence for continuous spectrum states. Now we consider one of the interesting features of oscillator basis.

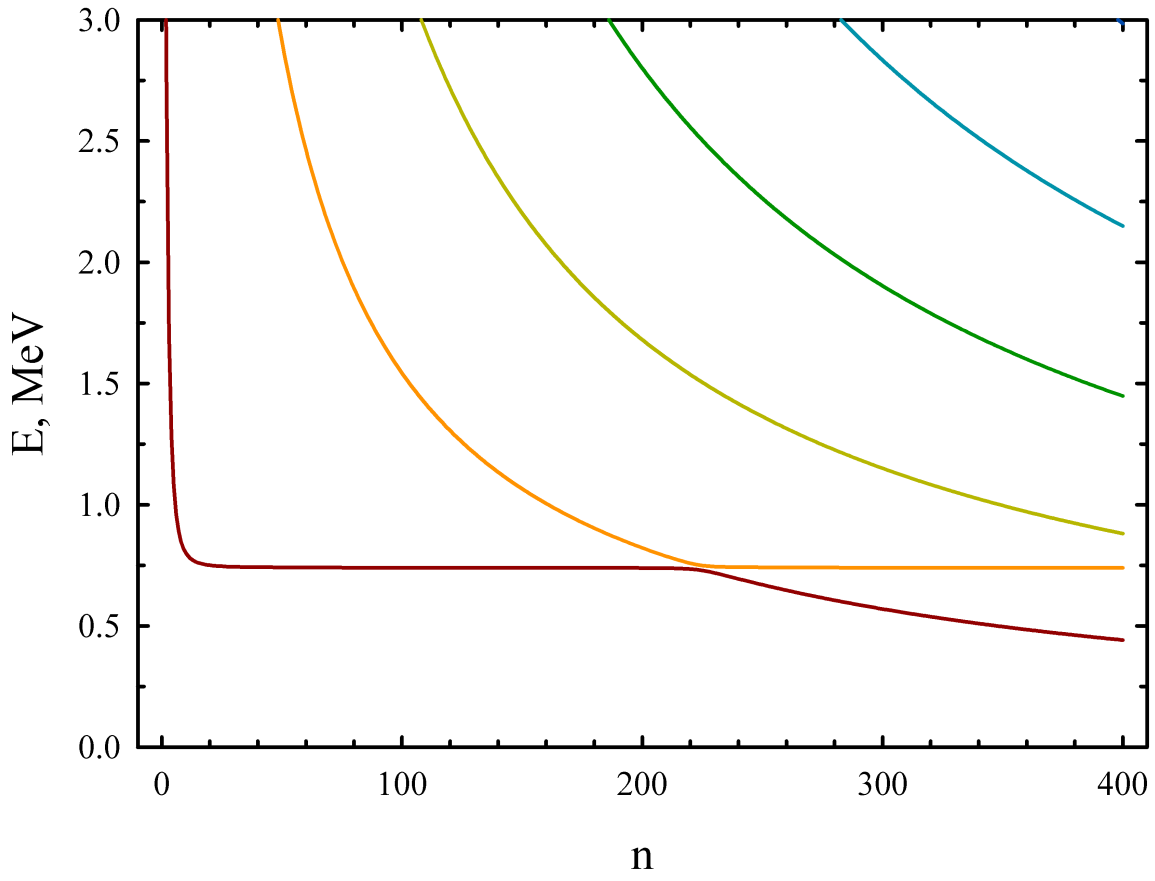

FIG. 12: Spectrum of the $7/2^-$ states in ^{7}Li as a function of the number of oscillator functions.

By investigating how spectrum of energies of two-cluster system depends on the number of oscillator functions, taking part in calculations, we can predict position (i.e. the energy) of narrow resonance state. For this aim, we consider the $7/2^-$ states in ^{7}Li and ^{7}Be. It is well known [56] that these nuclei have narrow resonances in the $7/2^-$ state. In Figures 12 and 13 we show spectrum the $7/2^-$ states in ^{7}Li and ^{7}Be, respectively, obtained with the

different number of oscillator functions.

Main feature of these figures, that there are plateaus, i.e. energy of some excited states is not changed when we increase the number of oscillator functions. These plateaus unambiguously indicate the position of resonance states. Such phenomenon was used in the Stabilization Method [98]. Many interesting examples of the realization of the stabilization method in light nuclei can be found in Ref. [47]. Note that it is very difficult to locate wide resonance states with such technique, as they exhibit themselves as some irregularities in a rather wide energy range in behavior of the energy as a function of n. The pictures 12 and 13 predict resonance state in ^{7}Li at energy approximately 0.75 MeV and in ^{7}Be at the energy about 1.75 MeV. To locate these resonance states we need less than 100 oscillator functions. One notices, that the plateau in ^{7}Li is more stable than the plateau in ^{7}Be.

We will see later, by considering phase shifts of ^{4}He + ^{3}H and ^{4}He + ^{3}He scattering, that such difference indicates that the $7/2^-$ resonance state in ^{7}Li is more narrow than the one in ^{7}Be.

VI. CONTINUOUS SPECTRUM STATES

In this section we consider states of the continuous spectrum. We will present phase shifts, partial and total cross sections of elastic scattering of clusters. Special attention will be paid to parameters of resonance states and to the structure of resonance wave functions.

A. Phase shifts

Phase shifts of the elastic scattering of neutrons from an alpha particle are shown in Figure 14. Phases shifts for $J^\pi = 3/2^-$ and $J^\pi = 1/2^-$, generated by the total orbital momentum $L = 1$, exhibit the resonance behavior. Phase shifts for the elastic $\alpha + d$ scattering for different values of the total orbital momentum L, the total angular momentum J and parity π are presented in Figure 15. One notices that phase shifts for negative parity states are very small. Calculated phase shifts indicated that there are three resonance states in ^{6}Li created by the Coulomb and centrifugal barriers. These resonance states are associated with the following channels: $J^\pi = 3^+$, $J^\pi = 2^+$ and $J^\pi = 1^+$.

In Figure 16 we display phase shifts of the elastic α+^{3}He scattering. Due to the Coulomb

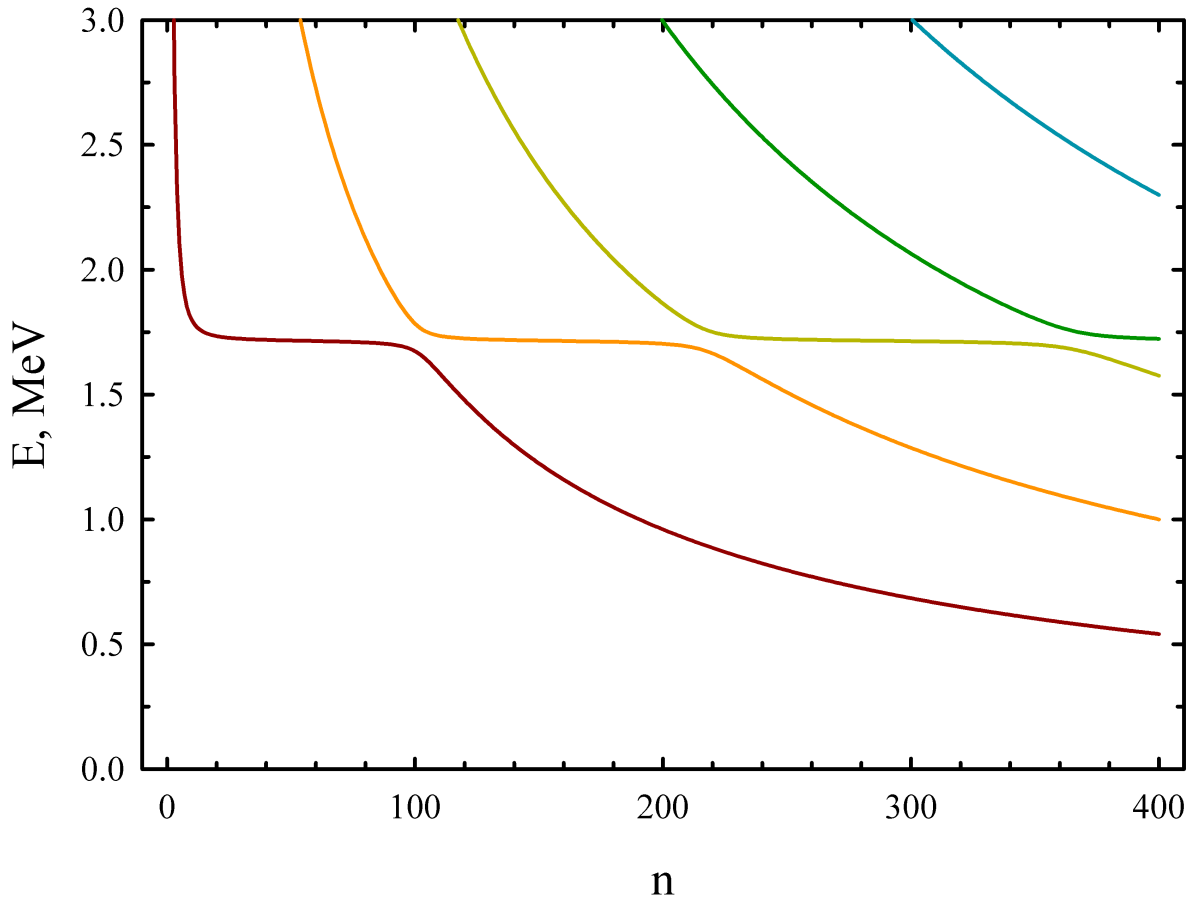

FIG. 13: Spectrum of the $7/2^-$ states in ^{7}Be as a function of number of oscillator functions.

interaction, phase shifts are very small at a rather large energy range $0 < E < 0.5$ MeV. Phase shifts for the negative parity state and for the total angular momentum $J = 7/2$ and $J = 5/2$ exhibit a resonance behavior. We can see that the $7/2^-$ resonance state is much narrow than the $5/2^-$ resonance state.

It is important to note the general feature in behavior of phase shifts for ^5He,^{5} Li,^{6} Li,^{7}Li and ^{7}Be nuclei. Within our model, these nuclei have both the negative and positive parity states, while ^{8}Be has only the positive parity states. The normal parity state $\pi = (-1)^A$ dominates in nuclei ^{5}He, ^{5}Li, ^{6}Li, ^{7}Li and ^{7}Be. It means that phase shifts of the normal parity state have large values and they usually exhibit resonance states.

Phase shifts of the abnormal parity states $\pi = (-1)^{A+1}$ are close to zero in the considered

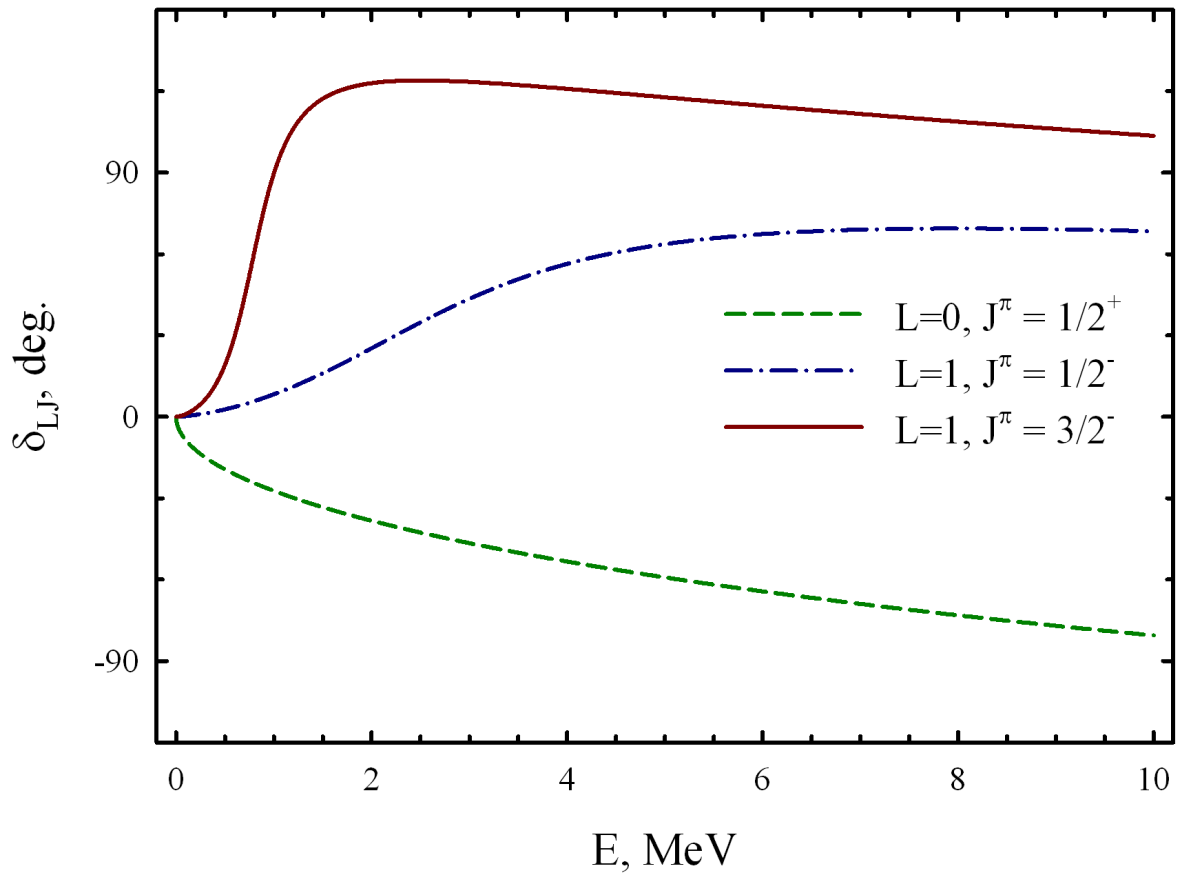

FIG. 14: The elastic phase shifts for the $n + \alpha$ scattering.

energy range. There is one exception from this rule. The s-wave phase shift ($L = 0$) in odd nuclei noticeable decreases with increasing of energy of scattering state. Figures 17 and 18, where we show obtained phase shifts and available experimental ones, demonstrate that our model describes fairly good the phase shifts in ^{5}Li and ^{8}Be, respectively.

Experimental data for $\alpha + p$ system is taken from Refs. [99], [100], [101], [102] and the experimental phase shifts for $\alpha + \alpha$ scattering are from Refs. [103] and [104].

B. Cross Sections

Let us start with ^{7}Li nucleus. The partial and total cross sections of elastic α+t scattering are display in Figure 19. One can see a huge and narrow peak created by the $7/2^-$ resonance

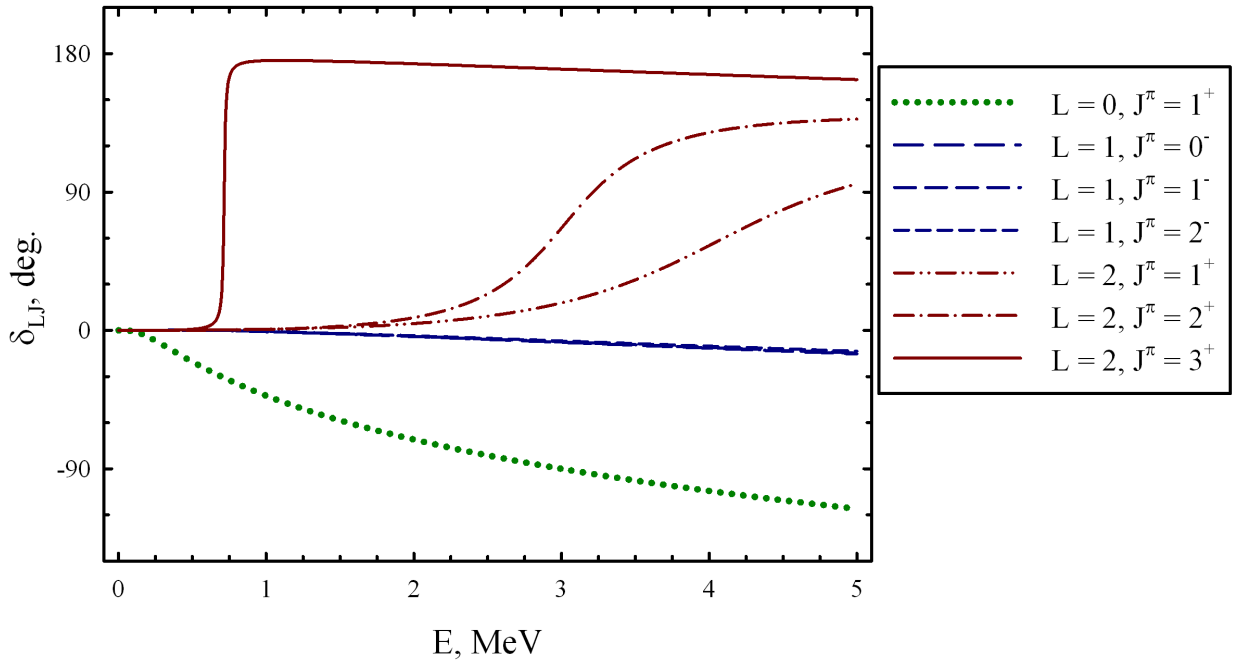

FIG. 15: The elastic phase shifts for the $d + \alpha$ scattering.

state. Meanwhile, contribution of the $5/2^-$ resonance state to the partial and total cross sections is not so prominent. Having calculated phase shifts $\delta_{LJ}(E)$, it is easy now to calculate partial cross sections $\sigma_{LJ}(E)$ and the total cross section $\sigma(E)$ which is determined as

$$\sigma(E) = \sum_{L,J} \sigma_{LJ}(E), \tag{19}$$

while a partial cross section $\sigma_{LJ}(E)$ is connected to the corresponding phase shift by the relation

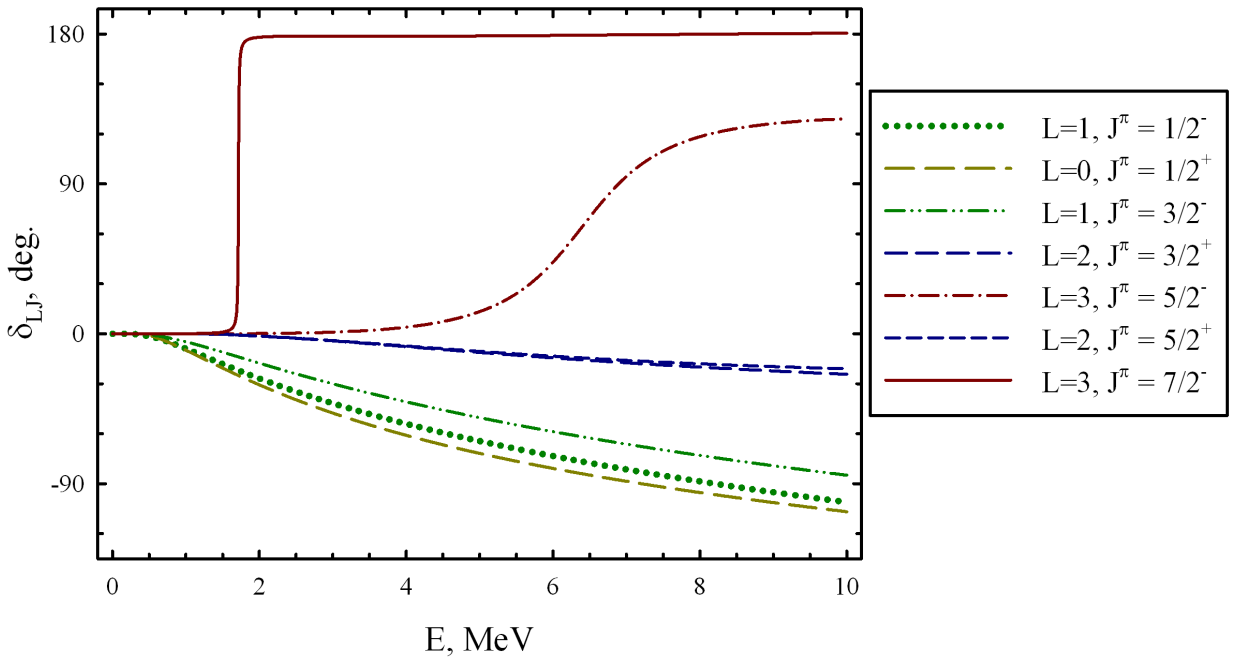

FIG. 16: Phase shifts of the elastic α+^{3}He scattering.

$$\sigma_{LJ}(E) = \frac{4\pi}{k^2} \sin^2 \delta_{L,J}(E), \tag{20}$$

where

$$k = \sqrt{2m\mu E}/\hbar, \quad \mu = \frac{A_1 A_2}{A_1 + A_2}. \tag{21}$$

It is interesting to compare cross sections for the $\alpha + t$ scattering (Figure 19) with those for the α+^{3}He scattering (Figure 20). The $7/2^-$ resonance state in ^{7}Be has also great impact on the partial and total cross sections of the elastic α+^{3}He scattering. However, contribution of the $7/2^-$ channel to the total cross section is very small outside the small region of the resonance state $7/2^-$. And this is observed for the α+^{3}He and $\alpha + t$ scattering. In both cases, the L=0 channel with quantum numbers $J^\pi = 1/2^+$ dominates at the low energy region $0 \geq E \geq 3$ MeV. This channel describes the head-on collision of two-clusters, i.e. interaction of two clusters with the zero value of the total orbital momentum $L = 0$.

At the low energy range ($0 \leq E \leq 0.4$ MeV for ^{7}Li and $0 \leq E \leq 0.8$ MeV for ^{7}Be), the total cross sections of the α+^{3}He and $\alpha + t$ scatterings are very small due to the Coulomb

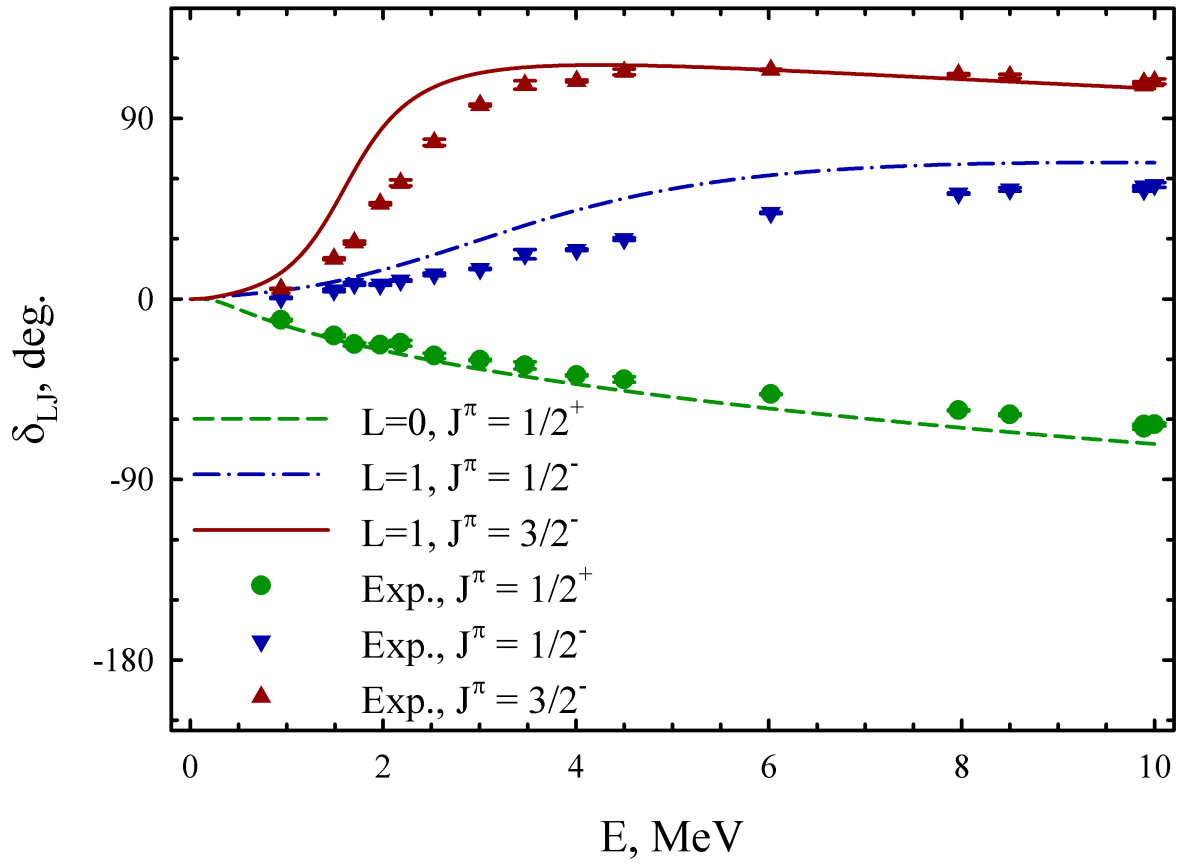

FIG. 17: Theoretical and experimental phase shifts for the elastic $\alpha + p$ scattering.

interaction.

C. Resonance States

Resonance states are very interesting phenomena in two- and many-cluster continuum. Present model allows us to study so-called the shape resonance states, it means resonance states created by the Coulomb or/and centrifugal barriers. These resonances lie close to the two-cluster decay threshold. Some of these resonances are members of rotational spectra. In this section we are going to study in detail parameters of resonance states and analyze their wave functions.

As we consider two pairs of mirror nuclei, namely ^{5}He and ^{5}Li, ^{7}Li and ^{7}Be, we will

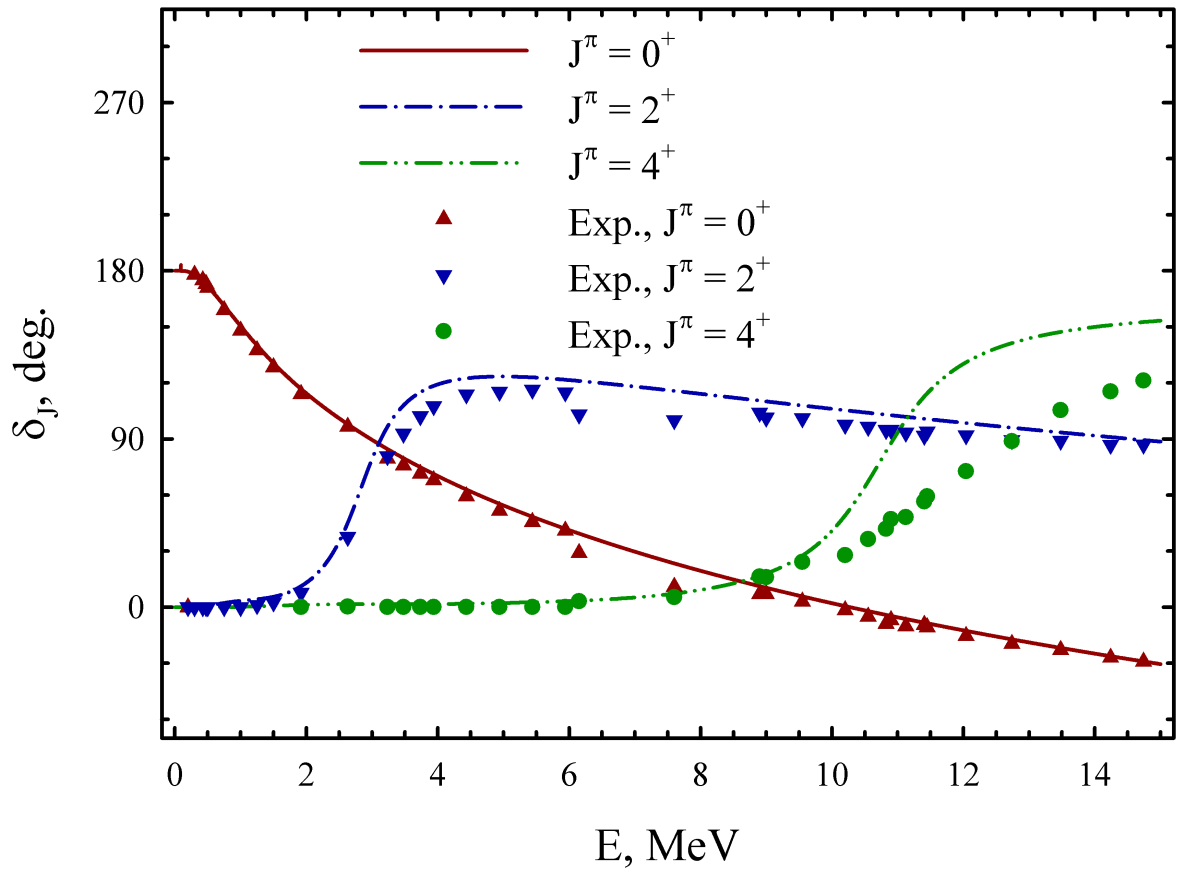

FIG. 18: Phase shifts of the elastic $\alpha + \alpha$ scattering, calculated within the present two-cluster model and compared with the corresponding experimental data.

investigate effects of the Coulomb interaction on energy and width of resonance states in these nuclei. In Table V we collect parameters of the narrow resonance states. In fact this Table includes three very narrow resonance states with the total width Γ from 1 to 17 keV, two rather wide resonance states. The later represent the ground state of ^{5}He and ^{5}Li, nuclei that have no bound states.

Let us consider wave functions of the selected resonance states. In Figure 21 we display wave functions of narrow resonance states ^{5}He, ^{5}Li, ^{6}Li, ^{7}Li and ^{7}Be, with quantum numbers indicated in Table V. Wave functions are represented in coordinate space and thus they depend on distance between clusters r. Main feature of these resonances is that their wave functions are concentrated at small distances, where interaction between cluster is very

TABLE V: Parameters of the most narrow resonance states in light nuclei.

Nucleus	J^π	E, MeV	Γ, MeV	E, MeV	Γ, MeV
^{5}He	$3/2^-$	0.782	0.679	-	-
^{5}Li	$3/2^-$	1.598	1.316	2.78± 0.03	-3.83± 0.03
^{6}Li	3^-	0.716	0.017	-	-
^{7}Li	$7/2^-$	0.741	0.001	2.78± 0.03	-3.83± 0.03
^{7}Be	$7/2^-$	1.716	0.012	-	-
^{8}Be	0^+	0.0932	$12.98 \cdot 10^{-6}$	0.0918	$(5.57 \pm 0.25) \cdot 10^{-6}$

TABLE VI: Parameters of broad resonance states in ^5He,^{5} Li,^{6} Li,^{7} Li,^{7}Be, ^{8}Be.

Nucleus	J^π	E, MeV	Γ, MeV	E, MeV	Γ, MeV
^{5}He	$1/2^-$	2.117	5.957	2.068	5.57
^{5}Li	$1/2^-$	2.996	7.297	3.18	6.60
^{6}Li	2^+	3.019	0.999	2.838±0.022	1.30±0.10
	1^+	4.056	2.331	4.176±0.050	1.5±0.20
^{7}Li	$5/2^-$	5.417	2.118	4.137	0.918
^{7}Be	$5/2^-$	6.398	2.025	5.143±0.10	1.2
^{8}Be	2^+	2.831	1.194	3.122±0.01	1.513±0.015
	4^+	10.73	1.925	11.442±0.15	3.50

strong.

We assume that the range of distance where wave function has a large amplitude is restricted by barrier, generated by centrifugal or Coulomb forces. Under and after barrier, resonance wave functions oscillate with small amplitude. This is a canonical behavior of resonance wave functions.

In Table VI we show parameters of the broad resonance states. The width of such resonance states varies from 1 to 7.3 MeV. In ^{5}He and ^{5}Li, width of the $1/2^-$ resonance states is substantially larger than their energy. It is important to stress, that parameters of resonance states in nuclei ^{5}He, ^{5}Li, ^{6}Li, ^{7}Li and ^{7}Be are strongly depends on intensity of the

spin-orbital forces.

Results, shown in Table VI, indicates that the combination of the centrifugal and Coulomb barriers creates a powerful barrier, which generates resonance states with energy up to 11 MeV.

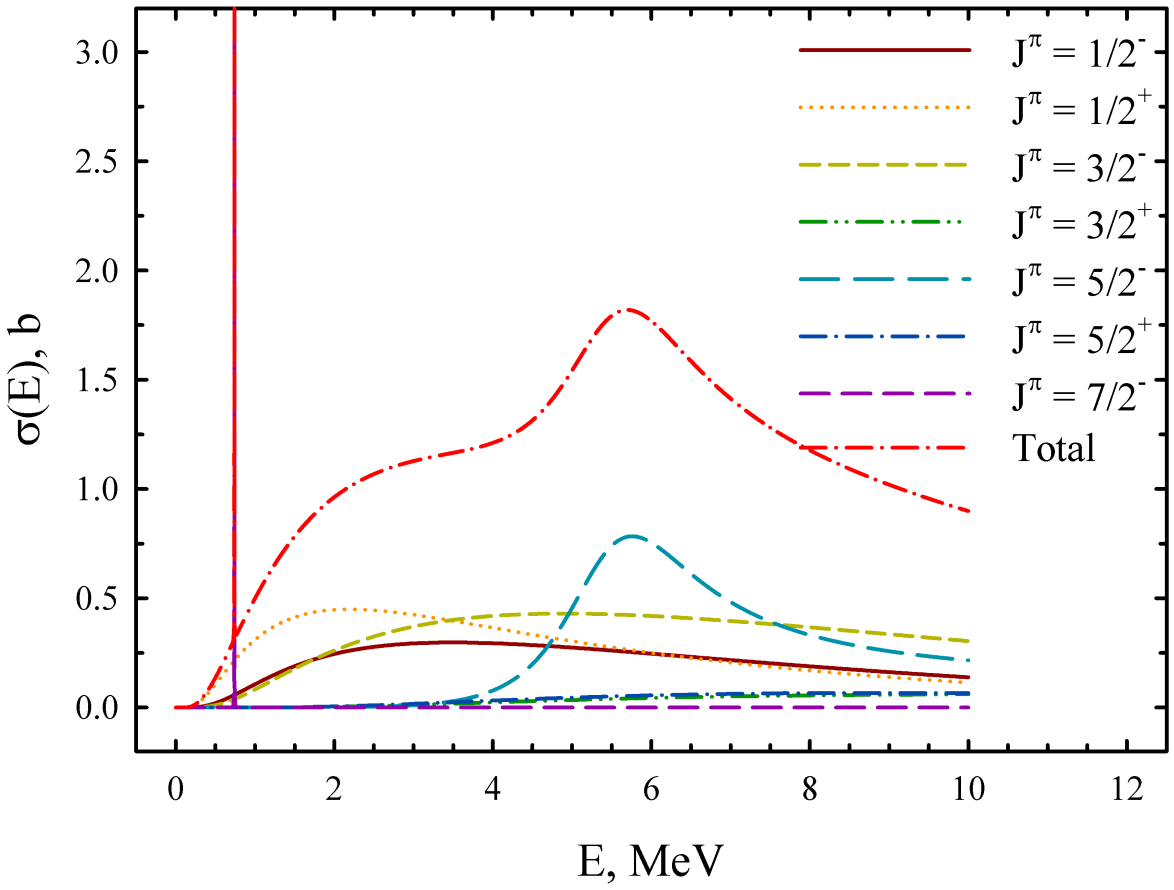

FIG. 19: Partial and total cross sections for the $\alpha + t$ elastic scattering.

To demonstrate how parameters of resonance states depends on the shape of a nucleon-nucleon potential, we select nucleus ^{8}Be and we made additional calculations by involving the Minnesota potential (MP) [105] and the Volkov potential N2 (VP) [106]. As for the MHNP, we select the oscillator length b to minimize the energy of an alpha particle, the exchange parameter u of the MP and the Majorana parameter m of the VP is chosen to reproduce energy of the 0^+ resonance state in ^{8}Be. The optimal parameters for the MP are $b = 1.285$ fm, $u = 0.9276$, and for the VP they equal $b = 1.376$ fm, $m = 0.6011$. Results

of these calculations are presented in Table VII. Energy of resonance states is determined with respect to the $\alpha + \alpha$ threshold energy. In Table VII we also compare results of our calculations with the available experimental data [57].

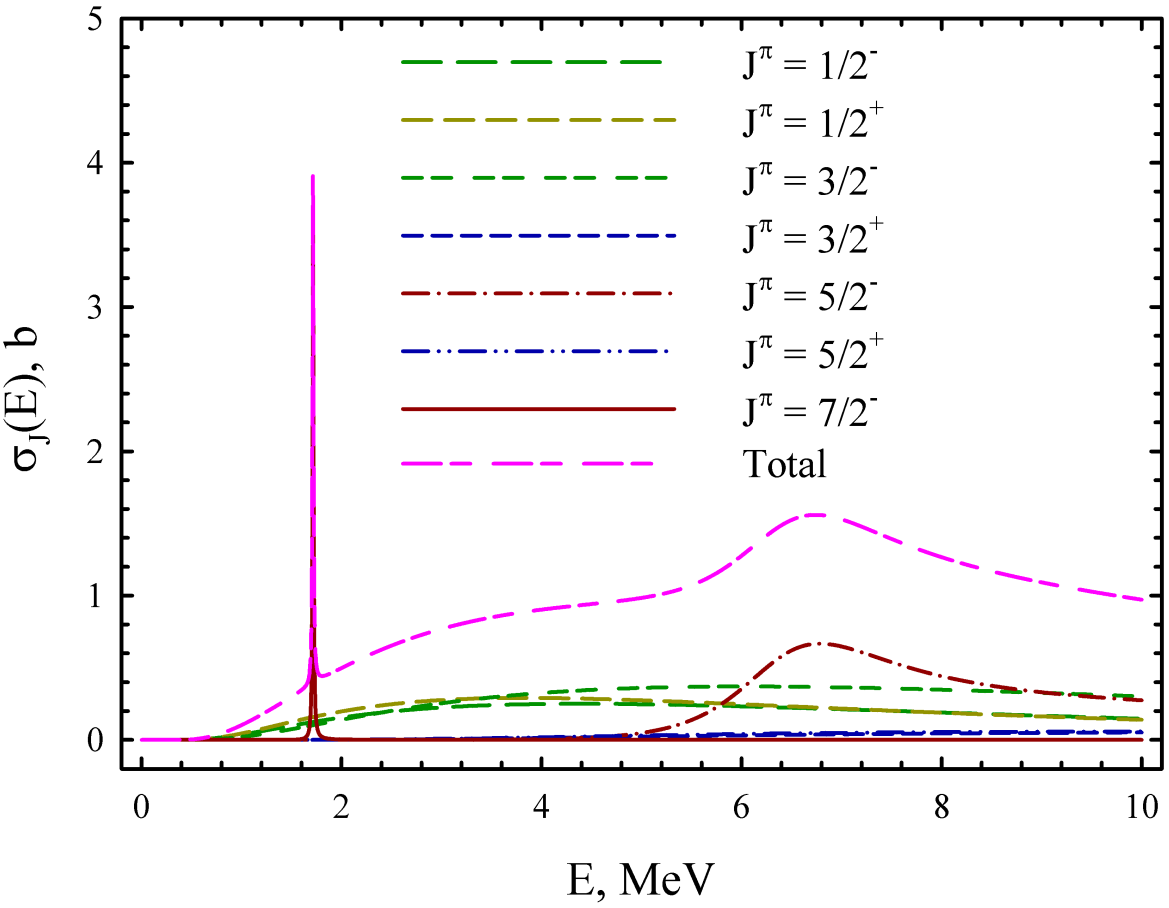

FIG. 20: The total and partial cross sections for the α + ^{3}He elastic scattering.

As one can see energy and width of the 2^+ and 4^+ resonance states, calculated with different nucleon-nucleon potentials, are rather different. Thus parameters of resonance states depend substantially on the shape of nucleon-nucleon interactions.

D. Folding potential

Let us evaluate the shape of the Coulomb barrier. Within the Resonating Group Method, a potential of cluster-cluster interaction is nonlocal, and thus it is difficult to analyze such

TABLE VII: Spectrum of resonance states in ^{8}Be, calculated with three different nucleon-nucleon potentials and compared with experimental data.

Potential	J^π	E, MeV	Γ, MeV	E_{exp}, MeV	Γ_{exp}, MeV
MHNP	0^+	0.093	$12.98 \cdot 10^{-6}$	0.092	$(5.57 \pm 0.25) \cdot 10^{-6}$
VP	0^+	0.091	$11.07 \cdot 10^{-6}$		
MP	0^+	0.092	$10.72 \cdot 10^{-6}$		
MHNP	2^+	2.820	1.196	3.122±0.01	1.513±0.015
VP	2^+	2.529	1.496		
MP	2^+	2.977	1.773		
MHNP	4^+	10.730	1.925	11.442±0.15	3.500
VP	4^+	10.856	6.734		
MP	4^+	12.779	5.615		

an object. In a two-cluster model, only the folding potential has more simple local form. It helps us to evaluate width and height of barrier created by the Coulomb forces. In Figure 22 we display folding potentials for all nuclei considered. They consist of the nucleon-nucleon part and Coulomb contribution. As we see the folding potentials are deep and attractive especially for nuclei ^{6}Li, ^{7}Li, ^{7}Be and ^{8}Be. There is a small repulsive core in ^{5}He and ^{5}Li. One can also see that the isobaric nuclei (^{5}He and ^{5}Li, ^{7}Li and ^{7}Be) have a very close folding potentials.

Lower part of Figure 23 shows the height of the Coulomb barrier. It is less than 1 MeV. It is interesting that asymptotic tail of folding potentials is the same for isotopes and is determined by the Coulomb forces.

From Figure 22 one can deduce that internal region is stretched from $r = 0$ to $r \leq 6fm$. The asymptotic region lies in the region $r > 6fm$, where the Coulomb interaction between clusters dominates. Such a definition of the internal and asymptotic regions is consistent with behavior of wave functions of the narrow resonance states (see Figure 21).

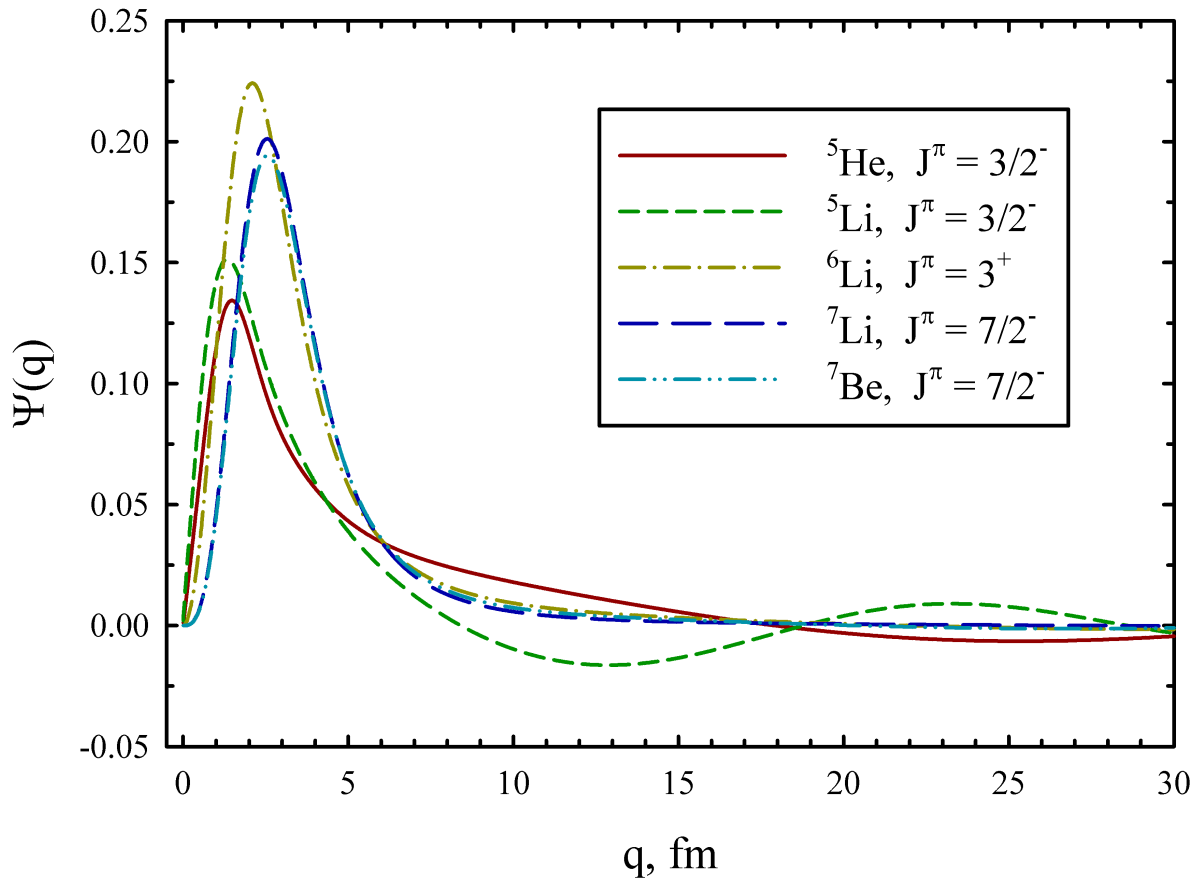

FIG. 21: Wave functions in the coordinate space of the most narrow resonance states for selected nuclei.

E. Effects of the Coulomb interaction

As we pointed out above, we selected the same input parameters for the mirror nuclei ^{5}He and ^{5}Li, ^{7}Li and ^{7}Be in order to study explicitly effects of the Coulomb interaction on the position of bound and resonance states, and on the width of resonance states as well. With such a choice of the input parameters difference in the position of bound and resonance states is totally determined by the Coulomb interaction.

In Figure 23 we show how the Coulomb interaction changes the energy of resonance states in ^{5}Li with respect to ^{5}He.

Figure 24 demonstrate effects of the Coulomb interaction on the spectrum of bound and

resonance states in ^{7}Li and ^{7}Be. As we can see, that the long-dashed lines in Figures 23 and 24, connecting corresponding states in mirror nuclei, are almost parallel. This indicates on similar effects of the Coulomb interaction on all bound and resonance states.

VII. CONCLUSIONS

We have investigated bound and resonance states in the lightest nuclei of the p-shell - ^{5}He, ^{5}Li, ^{6}Li, ^{7}Li, ^{7}Be and ^{8}Be. The Resonating Group Method was used to describe discrete and continuous spectrum states. These nuclei were considered as two-cluster systems with the dominant two-cluster configurations. The effective semi-realistic Hasegawa-Nagata potential was employed as a nucleon-nucleon interaction. The Majorana exchange parameter was slightly modified to reproduce energy of the ground state. Continuous spectrum of the negative and positive parity states was calculated with such a value of the Majorana parameter.

Energy and width of shape resonance states were calculated and compared with available experimental data. It was shown that our model describes fairly good the resonance structure of nuclei ^{5}He, ^{5}Li, ^{6}Li, ^{7}Li, ^{7}Be and ^{8}Be.

APPENDIX

1. Algebraic version of the Resonating Group Method

To study the nuclei in the framework of the Resonating Group Method (RGM), the complete wave function of the nucleus as a two-cluster system $A = A_1 + A_2$ is supposed to be sought in the following form

$$\Psi_J = \hat{A} \left\{ \left[\Phi_1(A_1) \Phi_2(A_2) \right]_S \psi^J_{LS}(q) Y_L(\hat{\mathbf{q}}) \right\}, \tag{22}$$

where $\hat{A}$ is the antisymmetrization operator; $\Phi_1(A_1)$ is the internal wave function of the A_1 nucleons of the first cluster, $\Phi_2(A_2)$ is the internal wave function of the A_2 nucleons of the second cluster, and $\psi^J_{LS}(q)$ is the wave function of the relative motion of the two clusters, depending on the Jacobi vector $\mathbf{q} = q \cdot \hat{\mathbf{q}}$. This Jacobi vector is proportional to the vector $\mathbf{r}$

$$\mathbf{q} = \mathbf{r} \sqrt{\frac{A_1 \cdot A_2}{A_1 + A_2}}, \tag{23}$$

where $\mathbf{r}$ determines the relative distance between the centers of mass of interacting clusters:

$$\mathbf{r} = \left[A_1^{-1} \sum_{i \in A_1} \mathbf{r}_i - A_2^{-1} \sum_{j \in A_2} \mathbf{r}_j \right], \tag{24}$$

$\mathbf{r}_i$ is the coordinate of the i-th nucleon ($i = 1,2, \ldots, A_1$) from the first cluster, and $\mathbf{r}_j$ is the coordinate of the j-th nucleon ($j = A_1 + 1, A_1 + 2, \ldots, A_1 + A_2$) from the second cluster.

In this work, we consider clusters of the s-shell, which means that the number of nucleons in each cluster A_1, A_2 should not exceed 4: $1 \leq A_1 \leq 4$, $1 \leq A_2 \leq 4$. The wave functions $\Phi_1(A_1)$ and $\Phi_2(A_2)$, describing the internal motion of nucleons inside both clusters, are fixed, they are constructed in the form of the Slater determinants from the oscillator functions of the translationally invariant shell model. Therefore, the functions $\Phi_1(A_1)$ and $\Phi_2(A_2)$ depend on the oscillator length b, which we define when performing numerical calculations. The functions $\Phi_1(A_1)$ and $\Phi_2(A_2)$ are chosen from the well-known multi-particle model of nuclear shells in the form of wave functions of the lowest, allowed states of the Pauli exclusion principle.

In the standard version of RGM, in order to find the wave function $\psi^J_{LS}(q)$ of the relative motion of clusters, it is necessary to solve the integro-differential equation. However, considering all the computational difficulties due to the presence of the antisymmetrization operator in the function, it will be much more convenient, instead of searching the explicit expression of $\psi^J_{LS}(q)$, to use the algebraic version of the RGM. The difference between this method and the classical RGM is that the classical version of the method is based on solutions of the integro-differential equation. Algebraic versions of the RGM circumvent such cumbersome calculations, simplifying and reducing them to a simple algebraic form, using the expansion of the inter-cluster function over the complete system of oscillator functions. A feature of the algebraic method is that the boundary conditions in the coordinate space for two or more cluster systems are transformed into a discrete oscillator space and are taken into account in dynamic equations. Thus, the algebraic form of the RGM is an exact realization of the matrix quantum theory possessing correct boundary conditions for descriptions of states of both continuous and discrete spectra.

The algebraic form of the RGM was proposed by Filippov [44], [45] and is effectively used to study the structure of nuclei. Using the algebraic version of the RGM, we decompose the wave function $\psi^J_{LS}(q)$ of the relative motion of clusters into a series of the complete set $\psi_n(q, b)$ of normalized radial oscillator functions in the coordinate space (radial wave

functions of a three-dimensional harmonic oscillator) [107–109]:

$$\Psi^J_{LS}(q) = \sum_{n=0}^{\infty} C_{nL;SJ}\ \psi_{nL}(q,b), \tag{25}$$

where q is the modulus of the vector $\mathbf{q}$ and

$$\psi_{nL}(q,b) = (-1)^n N_n b^{-3/2} \rho^L \exp\{-\rho^2/2\} L_n^{L+1/2}(\rho^2), \tag{26}$$

$$\rho = q/b, \quad N_n = \sqrt{\frac{2\Gamma(n+1)}{\Gamma(n+L+3/2)}}, \tag{27}$$

where n is the number of oscillator quanta (or nodes), b is the oscillator radius, $\Gamma(x)$ is the known gamma function [80], $L_n^{L+1/2}(z)$ is the generalized Laguerre polynomial, and $C_{nL;SJ}$ are the expansion or Fourier coefficients.

Similarly, from the topic itself, using the coefficients $C_{nL;SJ}$, we can expand the wave function $\psi^J_{LS}(p)$ in momentum space

$$\psi^J_{LS}(p) = \sum_{n=0}^{\infty} C_{nL;SJ}\ \psi_{nL}(p,b). \tag{28}$$

by employing oscillator functions in momentum space

$$\psi_{nL}(p,b) = N_n b^{3/2} \rho^L \exp\{-\rho^2/2\} L_n^{L+1/2}(\rho), \quad \rho = p \cdot b, \tag{29}$$

After that, the recording of formula (29) of the complete wave function of two cluster systems in the algebraic version of the RGM takes the form of a generalized Fourier series [45–48]. Then we can write

$$\Psi_J = \sum_{n=n_0}^{\infty} C_{nL;SJ}\ \Psi_{nL}, \tag{30}$$

where

$$\Psi_{nL} = \hat{A}\left\{[\Phi_1(A_1)\Phi_2(A_2)]_S\, \psi_{nL}(q,b) Y_L(\hat{q})\right\}. \tag{31}$$

Ψ_{nL} is the basis of many-particle oscillator functions, which is used to describe this cluster system of light nuclei, and the index is determined from the relation:

$$\begin{aligned}
n_0 &= 0 \quad \text{if } (L \geq A-3);\\
n_0 &= (A-L-4)/2 \ \text{ in the case of } (L \leq A-4) \text{ and } ((-1)^L = (-1)^A);\\
n_0 &= (A-L-3)/2 \ \text{ for } (L \leq A-3) \text{ and } ((-1)^L = (-1)^{A+1}.
\end{aligned}$$

The states with the minimal value of number n of oscillator quanta included in this basis correspond to those configurations of the nuclear shell model [110, 111], which are compared to the ground states of light nuclei. Consequently, the expansion according to the formula (30) takes into account not only the cluster, but also the shell configurations, which allows us to consider cluster systems without going beyond the limits adopted in the translationally invariant shell model [110, 111].

The oscillator functions Ψ_{nL} are completely antisymmetric and constitute a complete set of basis functions with specific physical properties. The number of these specific properties include belonging to the Hilbert space describing $A_1 + A_2$ clustering of the system of A nucleons with fixed internal cluster functions $\Phi(A_1)$ and $\Phi(A_2)$. In the algebraic version of the RGM, finding the wave function of the relative motion of clusters $\psi^J_{LS}(q)$ reduces to the problem of finding the unknown coefficients of the expansion of $C_{nL;SJ}$. The Fourier coefficients $C_{nL;SJ}$, representing the wave function of the relative motion of two clusters in a discrete oscillator representation, satisfy the system of linear algebraic equations [45, 47, 48]

$$\sum_{m=n_0}^{\infty} \left[\left\langle \Psi_{nL} | \hat{H} | \Psi_{mL} \right\rangle - E \left\langle \Psi_{nL} | \Psi_{mL} \right\rangle \right] C_{mL} = 0, \tag{32}$$

where $\left\langle \Psi_{nL} | \hat{H} | \Psi_{mL} \right\rangle$ are the matrix elements of the Hamiltonian between the cluster oscillator functions. The Dirac brackets mean an integration over spatial coordinates and a summation over the spin and isospin variables of all nucleons. $\langle \Psi_{nL} | \Psi_{mL} \rangle = \delta_{nm} \lambda_n$ is the normalization kernel or the overlap integral of the oscillator functions [48]. λ_n are the eigenvalues of the antisymmetrization operator. For $\lambda_n = 0$, the state Ψ_{nL} is a forbidden Pauli state. Such states do not participate in the construction of the wave function (29) and do not describe the dynamics of the two-cluster system. To do this, only the states allowed by the Pauli principle are used, for which $\lambda_n > 0$.

The antisymmetrization operator $\hat{A}$ influences the normalization of the oscillator functions, and the basis functions and the Fourier coefficients should be renormalized as follows

$$|\bar{n}L >= \frac{|\Psi_{nL} >}{\sqrt{\lambda_n}}, \quad |\bar{m}L >= \frac{|\Psi_{mL} >}{\sqrt{\lambda_n}}, \quad \bar{C}_{mL} = \frac{C_{mL}}{\sqrt{\lambda_n}}. \tag{33}$$

Thus, we arrive at the standard matrix form of the Schrödinger equation with an orthonormal basis of functions and obtain an infinite system of linear homogeneous algebraic equations

of the form [45, 47, 48]

$$\sum_{m=n_0}^{\infty} \left[\left\langle \bar{n}L|\hat{H}|\bar{m}L \right\rangle - E\delta_{n,m} \right] \bar{C}_{mL} = 0, \tag{34}$$

where $\hat{H}$ is a many-particle Hamiltonian of the nucleus, E is the total energy of the nuclear system, $\left\langle \bar{n}L|\hat{H}|\bar{m}L \right\rangle$ are matrix elements of the Hamiltonian between oscillator functions Ψ_{nL}. The indices n and m enumerate only the states allowed by the Pauli principle.

The expansion of the total wave function for the two-cluster system (30) contains an infinite set of basis functions. However, we need only a limited set of basis functions from it. For the oscillator representation this situation is analogous to the coordinate form of the Schrödinger equation, where it is required to find the wave function only up to a certain finite distance R_a. Outside this point, the well-known form of the asymptotic wave function is valid. And the value of R_a determines the distance at which the short-range interaction will be negligibly small and the asymptotic part of the Hamiltonian will be dominant. The same principle will be true for a discrete representation. Thus, it is necessary to calculate the wave function up to a finite value $n = N_a$. Starting from this quantum number, the asymptotic form will be valid for the coefficients of the expansion of the wave function. Like R_a, the parameter N_a sets the boundary between the inner and asymptotic regions. Thus, in the numerical solution of the Schrödinger equation both in the oscillator and in the coordinate representation, the parameters R_a and N_a are used as variational parameters. Thus, in order that their further increase does not change the results of the calculations, it will be necessary to determine their minimum values.

To solve the system of equations (32) and (34), it will be necessary to take into account the corresponding boundary conditions. The asymptotic form of the wave function of the bound state in the coordinate space (valid for large values of $q >> 1$) is [45, 47, 48]:

$$\psi(q) \approx \exp -kq/q, \quad k = \sqrt{2mE}/\hbar. \tag{35}$$

In the oscillator representation, the asymptotic form of the expansion coefficients C_{nL} for the bound state for $n >> 1$ has the form [45–48]

$$C_{nL} \approx \sqrt{R_n} \exp\left(-kbR_n\right)/R_n, \quad R_n = \sqrt{4n + 2L + 3}. \tag{36}$$

Similar relations are valid for the wave function of the continuous spectrum (the case of a single channel) in the coordinate space [45–48]:

$$\psi(q) \approx \sin\left(kq + \delta_l + L\pi/2\right)/q, \tag{37}$$

and also in the oscillator representation:

$$C_{nL} \approx \sqrt{R_n} \sin\left(kbR_n + \delta_L + L\pi/2\right)/R_n, \tag{38}$$

where δ_L is the scattering phase.

Equations (35) - (38) show the asymptotic form of the wave functions of the relative motion of clusters. With their help, it is possible to construct a closed system of equations that includes the correct boundary conditions for states of the discrete and continuous spectrum. How this is realized, we will show for states of the continuous spectrum. For simplicity of exposition, suppose that we have neutral clusters or, what is the same thing, that we "turned off" the Coulomb interaction between protons. The procedure that we are going to present is analogous to the procedure used in the coordinate space in quantum mechanics for two interacting particles. We recall its main stages. When the distance between the particles is large, we can neglect the interaction (it is negligible small in the asymptotic region), and the Hamiltonian will be represented only by the kinetic energy operator. In this case the Schrödinger equation has two linearly independent solutions $\psi_{kL}^{(R)}$ and $\psi_{kL}^{(I)}$, a regular and irregular one correspondingly:

$$\psi_{kL}^{(R)} = \sqrt{\frac{2}{\pi}} k \; j_L(kq), \quad \psi_{kL}^{(I)} = \sqrt{\frac{2}{\pi}} k \; n_L(kq), \tag{39}$$

where $j_L(kq)$ and $n_L(kq)$ are the spherical Bessel and Neumann functions, respectively (see their definition, for example, in [80]). Consequently, the asymptotic solution $\psi_{kL}^{(a)}$ of the Schrödinger equation for two particles or two clusters with a short-range potential will be a superposition of these two functions:

$$\psi_{kL}^{(a)} = \psi_{kL}^{(R)} - \tan(\delta_L) \; \psi_{kL}^{(I)} = \sqrt{\frac{2}{\pi}} k \left[j_L(kq) - \tan(\delta_L) \; n_L(kq) \right]. \tag{40}$$

By matching this asymptotic solution with a solution in the internal region at the point R_α, we obtain the wave function and the scattering phase shift for the state of the continuous spectrum with the orbital angular momentum L and energy E.

In the oscillator representation, the same idea is used. The expansion coefficients $(C_{0L}, C_{1L}, ..., C_{N_a L})$ describe the internal part of the wave function, and the coefficients

$$C_{\nu L}^{a} = C_{\nu L}^{(R)} - \tan(\delta_L) \; C_{\nu L}^{(I)}, \quad \nu > N_a, \tag{41}$$

represent its asymptotic part. Analytic expressions and the asymptotic form of the coefficients of the expansion $C_{nL}^{(R)}$ and $C_{nL}^{(I)}$ of both regular and irregular solutions are presented,

for example, in [83], [82],[44], [112]. Note that the asymptotic form of the coefficients $C^a_{\nu L}$ coincides with formula (38).

Taking into account the decomposition of the expansion coefficients into the internal and asymptotic parts and also taking into account the form for the asymptotic part of the expansion coefficients, we rewrite the system of equations (32) as follows

$$\sum_{m=n_0}^{N_a}\left[\left\langle \bar{n}L|\hat{H}\bar{m}L\right\rangle - E\delta_{nm}\right]\bar{C}_{mL} - \tan\delta_L\cdot\left\langle \bar{n}L|\hat{H}|N_a+1,L\right\rangle C^I_{N_a+1,L} = \\ -\left\langle \bar{n}L|\hat{H}|N_a+1,L\right\rangle C^{(R)}_{N_a+1,L}. \tag{42}$$

As a result, we obtain an inhomogeneous system of linear algebraic equations, into which the boundary conditions are explicitly included and whose solutions give us the phase shift of scattering and the wave function of the continuous spectrum in the oscillator representation.

For the expansion (29), we can write an equivalent formula for the inter-cluster wave function, using similar sets of expansion coefficients [45–48]

$$\psi^J_{LS}(q) = \sum_{n=0}^{\infty} C_{nL}\psi_{nL}(q,b). \tag{43}$$

A similar formula can be used to determine the inter-cluster function $\psi^J_{LS}(p)$ of momentum space. The functions $\psi^J_{LS}(q)$ and $\psi^J_{LS}(p)$ are connected by the Fourier-Bessel transformation

$$\psi^J_{LS}(p) = \sqrt{\frac{2}{\pi}}\int_0^{\infty} q^2 dq j_L(pq)\phi^J_{LS}(q). \tag{44}$$

Having calculated the scattering phase shifts, we can use them to obtain the parameters of the resonant states, that is, to determine their energy and width. The energy and width for the resonance are determined using the relations [113]

$$\frac{d^2\delta}{dE^2}|_{E=E_r} = 0, \quad \Gamma = 2(\frac{d\delta}{dE})^{-1}|_{E=E_r}. \tag{45}$$

The scattering phases in the vicinity of an isolated resonance can be represented as the sum of the background and resonant scattering phases. For the resonant scattering phase shift we use the Breit-Wigner formula [114–117]:

$$\delta(E) = \delta_b(E) + \delta_r(E) = \delta_b(E) - \arctan(\Gamma_r/2\cdot(E-E_r)). \tag{46}$$

Here, $\delta_b(E)$ is the background phase shift, $\delta_r(E)$ is the resonant phase shift, E_r and Γ_r are the energy and width of the resonant state. The first derivative of the scattering phase shift

$\delta(E)$ with respect to energy E is

$$\frac{d\delta(E)}{dE} = \frac{d\delta_b(E)}{dE} + \frac{2\Gamma}{4(E-E_r)^2 - \Gamma^2}$$

Assuming that the first derivative of the background phase shift with respect to the energy is much smaller than the first derivative of the resonant scattering phase, we obtain

$$\frac{d\delta(E)}{dE} \approx \frac{2\Gamma}{4(E-E_r)^2 + \Gamma^2}.$$

This equation means that $d\delta(E)/dE$ as a function of energy has a minimum at $E = E_r$ and this minimum equals to

$$\left.\frac{d\delta(E)}{dE}\right|_{E=E_r} = \frac{2}{\Gamma}. \tag{47}$$

To find minimum of the function $d\delta(E)/dE$, one can use the following criterion:

$$\left.\frac{d^2\delta(E)}{dE^2}\right|_{E=E_r} = 0. \tag{48}$$

Eqs. (47) and (48) justify the relations (45).

Using the representation (46) for the total scattering phase, we obtain the following expression for the elastic scattering cross-section in the vicinity of the resonance

$$\sigma(E) = \frac{\pi}{k^2}|S(E) - 1|^2 = \sigma_{res}(E) + \sigma_b(E) + \sigma_{res,b}. \tag{49}$$

Here, the cross section of resonance scattering is

$$\sigma_{res}(E) = \frac{\pi}{k^2}\left\{\frac{\Gamma^2}{(E-E_r)^2 + \Gamma^2/4}\right\}, \tag{50}$$

the background scattering cross-section is

$$\sigma_b(E) = 4\frac{\pi}{k^2}\sin^2(\delta_b(E)), \tag{51}$$

and the term determines the interference of resonance and background scattering can be written as:

$$\sigma_{res,b} = 2\Gamma\frac{\pi}{k^2}Re\left[\frac{\sin(\delta_b(E))e^{i\delta_b(E)}}{E - E_r + i\Gamma/2}\right]. \tag{52}$$

2. Program description

The program 2cl_SpectrPhases.exe is designed to calculate the Hamiltonian of a two-cluster system, the spectrum and wave functions of bound and pseudo-bound states, as well as scattering phase shifts.

The calculations are performed as follows:

1. The program calculates the matrix of the kinetic energy operator between the functions of the oscillator basis, then the matrix of the potential energy operator, which consists of the central and spin-orbit nucleon-nucleon interactions, and also with the Coulomb interaction. The spin-orbit interaction does not take part in the process if the total orbital angular momentum L or the total spin S of the nucleus are equal to zero.

2. Sum of the matrix of the kinetic and potential energy makes the matrix of the Hamiltonian.

3. Then the eigenvalues and eigen-functions of the Hamiltonian are calculated. The negative eigenvalues of the Hamiltonian determine the energy of bound states or a bound state if such a state exists. The corresponding eigen-functions determine the wave functions of the bound states of the nucleus in the oscillator representation. The positive eigenvalues and the corresponding eigenvectors represent the states of the continuous spectrum of a given nucleus.

4. 4. After that, the program builds the wave functions of the mutual motion of the clusters in the coordinate and momentum spaces.

5. 5. At the next stage, the program calculates the rms proton, neutron and mass radii, as well as quadrupole moments. Quadrupole moments are calculated for a state of the nucleus with the total angular momentum $J \geq 1$.

6. At the last stage the program calculates the phase shift of the elastic cluster-cluster scattering. With the aid of a simple procedure, the energy and width of the resonant state are determined from the scattering phase shift, provided that the resonance in the given nucleus and with this total angular momentum exists.

To perform the calculations, one needs to set the following input parameters in the configuration file "2cl_calc_spec.cfg":

1. lm is the orbital angular momentum;

2. tot_spin - the total spin of the system (the possible values of this parameter are given in Table VIII);

3. tot_mom - total angular momentum of the system;

4. n_ob_funs - the number of basic functions;

5. r_0 is the oscillator radius;

6. $select\_r0$. If select $select\_r0 = 'Opt'$, then the program finds the optimal value of r_0, which minimizes the energy of the two-cluster threshold, and calculates with it. If select $select\_r0 = 'Fix'$, then the calculation will be performed with the value of the oscillator radius r_0, which was entered in the previous line.

7. $npot$ - Number of the potential.

8. Majorana parameter is $majoran$. One can set $majoran = 0$ and use the original value of the parameter for all nucleon-nucleon potentials but the Minnesota potential. For the Minnesota potential one can use the value $majoran = 1$, which is mostly used value of the parameter. The Majorana parameter is often selected in such a way as to reproduce the experimental value of the ground state energy of the compound nucleus.

9. $Coulomb\_YN$ specifies: it is necessary ($Coulomb\_YN =' Y'$) or it is not necessary ($Coulomb\_YN =' N'$) to take into account the Coulomb. This parameter makes it possible to study explicitly the role of the Coulomb interaction on the states of the discrete and continuous spectrum.

10. ls_factor is a multiplier that changes the intensity of spin-orbital forces. This parameter is also used as an adjustable parameter. With its help, for example, it is possible to reproduce the experimental difference between the energies of the ground $3/2^-$ and the first excited $1/2^-$ states in the ^{7}Li and ^{7}Be nuclei.

11. $nucleus$ is name of a nucleus. The possible values of $nucleus$ are: '5He', '5Li', '6Li', '7Li', '7Be', '8Be' (see also Table VIII).

12. na is the number of nucleons in the nucleus (see Table VIII).

TABLE VIII: Key inpur parameters.

nucleus	5He	5Li	6Li	7Li	7Be	8Be
na	5	5	6	7	7	8
tot_spin	0.5	0.5	1.0	0.5	0.5	0.0
Clu_name_1	4He	4He	4He	4He	4He	4He
Clu_name_2	n	p	d	3H	3He	4He

TABLE IX: List of nucleon-nucleon potentials.

npot	name of potentail	sorce
1	modified Hasegawa-Nagata	[87, 88]
2	Volkov N1	[106]
3	Volkov N2	[106]
4	Brink-Boeker N1	[118]
5	Brink-Boeker N2	[118]
6	Minnesota	[105]

13. *Clu_name_*1 is the name of the first cluster ('4He') (see also Table VIII).

14. *Clu_name_*2 - the name of the second cluster. (*Clu_name_*2 = 'n', 'p', 'd', '3H', '3He', '4He'.) There should be three entries for the cluster name.) (See also Table VIII).

15. *E_ini*, *E_fin*, *E_step* - parameters that determine the energy interval in which the scattering phase shift will be calculated: initial energy *E_ini*, final energy *E_fin* and energy step *E_step*.

In Table IX we show a list of nucleon-nucleon potentials which can be used for calculations of two-cluster systems.

We have to select the only one free parameter of the model - the oscillator length b. We chose the oscillator length to minimize the energy of the two-cluster threshold. Such a choice provides an optimal description of the internal structure of alpha-particle in the ^{5}He, ^{5}Li and ^{8}Be nuclei. For ^{6}Li, ^{7}Li and ^{7}Be nuclei, the optimal value of oscillator length b allows us to describe in average the internal structure of the cluster pairs: α and d, α and t, α and ^{3}He, respectively.

To describe the nucleon-nuclear interaction, we will use the modified Hasegawa-Nagata potential (MHNP), for this purpose in the program *npot* is set to $npot = 1$. We take a Gaussian wave function as a one-particle wave function in the form: $f(x) = \exp(-x^2)$. This is the wave function of the ground state of a quantum harmonic oscillator and, therefore, is appropriate for any system around a potential minimum. In addition, the Gaussian form of wave functions and NN potential allows one to make all integrations in analytical form, which simplifies significantly the calculations. The Gaussian we use are real, which also reduces the number of terms that need to be calculated, since the rectilinear and inverse matrix elements are almost always the same.

The modified Hasegawa-Nagata potential for a pair nucleon-nucleon interaction reproduces fairly the attraction at large distances and the repulsion at short distances. The coordinate dependence of this potential takes the form of a superposition of a Gaussian. It is used in many cases, particularly, to describe the scattering of light nuclei over a wide range of energies. It can be seen in Figure 25, where we display the most strong, even components of the MHNP.

The Majorana exchange operator produces the exchange of spatial coordinates between two nucleons. The Bartlett exchange operator, describes the Wigner forces, which produce an exchange of spin variables between two nucleons. The Heisenberg exchange operator is an operator of NN forces that produce a simultaneous exchange of spin, isospin, and spatial coordinates. See more details about the static nucleon-nucleon potentials in Ref. [26].

To be more consistent with the experimental situation, we slightly change the Majorana parameter m of the Hasegawa-Nagata potential to reproduce position of the ground states of nuclei ^{6}Li, ^{7}Li and ^{7}Be and lowest resonance states in ^{5}He, ^{5}Li and ^{8}Be with respect to dominant two-cluster threshold. It is done in order to demonstrate that modifications are rather small.

References

[1] H. Horiuchi, K. Ikeda, and K. Katō, "Recent Developments in Nuclear Cluster Physics," *Prog. Theor. Phys. Suppl.*, vol. 192, pp. 1–238, 2012.

[2] M. Freer, "Clustering in Light Nuclei; from the Stable to the Exotic," in *Lecture Notes in*

Physics, Berlin Springer Verlag (C. Scheidenberger and M. Pfützner, eds.), vol. 879 of *Lecture Notes in Physics, Berlin Springer Verlag*, p. 1, 2014.

[3] M. Freer, H. Horiuchi, Y. Kanada-En'yo, D. Lee, and U.-G. Meißner, "Microscopic Clustering in Nuclei," *ArXiv e-prints*, May 2017.

[4] C. Beck, "Recent Experimental Results on Nuclear Cluster Physics," *ArXiv e-prints*, Aug. 2016.

[5] C. Beck, "From the stable to the exotic: clustering in light nuclei," *ArXiv e-prints*, Mar. 2016.

[6] C. Beck, ed., *Clusters in Nuclei, Volume 3*, vol. 875 of *Lecture Notes in Physics, Berlin Springer Verlag*, 2014.

[7] W. von Oertzen, M. Freer, and Y. Kanada-En'yo, "Nuclear clusters and nuclear molecules," *Phys. Rep.*, vol. 432, pp. 43–113, Sept. 2006.

[8] M. Kimura and H. Horiuchi, "Introduction of the deformed base AMD and application to the stable and unstable nuclei," *Nucl. Phys. A*, vol. 722, pp. 507–+, July 2003.

[9] A. Aprahamian, K. Langanke, and M. Wiescher, "Nuclear structure aspects in nuclear astrophysics," *Progr. Parti. Nucl. Phys.*, vol. 54, pp. 535–613, Apr. 2005.

[10] A. Coc, C. Angulo, E. Vangioni-Flam, P. Descouvemont, and A. Adahchour, "Big Bang nucleosynthesis, microwave anisotropy, and the light element abundances," *Nucl. Phys. A*, vol. 752, pp. 522–531, Apr. 2005.

[11] F. Iocco, G. Mangano, G. Miele, O. Pisanti, and P. D. Serpico, "Primordial nucleosynthesis: From precision cosmology to fundamental physics," *Phys. Rep.*, vol. 472, pp. 1–6, Mar. 2009.

[12] P. Descouvemont, A. Adahchour, C. Angulo, A. Coc, and E. Vangioni-Flam, "Compilation and R-matrix analysis of Big Bang nuclear reaction rates," *Atomic Data and Nuclear Data Tables*, vol. 88, pp. 203–236, Sept. 2004.

[13] E. G. Adelberger, S. M. Austin, J. N. Bahcall, A. B. Balantekin, G. Bogaert, L. S. Brown, L. Buchmann, F. E. Cecil, A. E. Champagne, L. de Braeckeleer, C. A. Duba, S. R. Elliott, S. J. Freedman, M. Gai, G. Goldring, C. R. Gould, A. Gruzinov, W. C. Haxton, K. M. Heeger, E. Henley, C. W. Johnson, M. Kamionkowski, R. W. Kavanagh, S. E. Koonin, K. Kubodera, K. Langanke, T. Motobayashi, V. Pandharipande, P. Parker, R. G. Robertson, C. Rolfs, R. F. Sawyer, N. Shaviv, T. D. Shoppa, K. A. Snover, E. Swanson, R. E. Tribble, S. Turck-Chièze, and J. F. Wilkerson, "Solar fusion cross sections," *Rev. Mod. Phys.*, vol. 70, pp. 1265–1291,

Oct. 1998.

[14] E. G. Adelberger, A. García, R. G. H. Robertson, K. A. Snover, A. B. Balantekin, K. Heeger, M. J. Ramsey-Musolf, D. Bemmerer, A. Junghans, C. A. Bertulani, J.-W. Chen, H. Costantini, P. Prati, M. Couder, E. Uberseder, M. Wiescher, R. Cyburt, B. Davids, S. J. Freedman, M. Gai, D. Gazit, L. Gialanella, G. Imbriani, U. Greife, M. Hass, W. C. Haxton, T. Itahashi, K. Kubodera, K. Langanke, D. Leitner, M. Leitner, P. Vetter, L. Winslow, L. E. Marcucci, T. Motobayashi, A. Mukhamedzhanov, R. E. Tribble, K. M. Nollett, F. M. Nunes, T.-S. Park, P. D. Parker, R. Schiavilla, E. C. Simpson, C. Spitaleri, F. Strieder, H.-P. Trautvetter, K. Suemmerer, and S. Typel, "Solar fusion cross sections. II. The pp chain and CNO cycles," *Rev. Mod. Phys.*, vol. 83, pp. 195–246, Jan. 2011.

[15] K. G. Balasi, K. Langanke, and G. Martínez-Pinedo, "Neutrino-nucleus reactions and their role for supernova dynamics and nucleosynthesis," *Progr. Part. Nucl. Phys.*, vol. 85, pp. 33–81, Nov. 2015.

[16] C. A. Bertulani and T. Kajino, "Frontiers in nuclear astrophysics," *Progr. Part. Nucl. Phys.*, vol. 89, pp. 56–100, July 2016.

[17] R. H. Cyburt, B. D. Fields, K. A. Olive, and T.-H. Yeh, "Big bang nucleosynthesis: Present status," *Rev. Mod Phys.*, vol. 88, p. 015004, Jan. 2016.

[18] H. Schatz, "Trends in nuclear astrophysics," *J. Phys. G Nucl. Phys.*, vol. 43, p. 064001, June 2016.

[19] J. M. Blatt and V. F. Weisskopf, *Theoretical Nuclear Physics.* New York, Berlin: Springer-Verlag, 1979.

[20] J. M. Eisenberg and W. Grenier, *Nuclear Theory. 1. Nuclear Models.* Amsterdam: North Holland, 1987.

[21] J. M. Eisenberg and W. Grenier, *Nuclear Theory. 2. Excitation mechanisms of the nucleus.* Amsterdam: North Holland, 1988.

[22] J. M. Eisenberg and W. Grenier, *Nuclear Theory. 3. Microscopic theory of the nucleus.* Amsterdam: North Holland, 1976.

[23] A. D. Shalit and H. Feshbach, *Theoretical Nuclear Physics. Volume I. Nuclear Structure.* New York: J. Wiley, 1990.

[24] H. Feshbach, *Theoretical Nuclear Physics. Volume II. Nuclear Reactions.* New York: J. Wiley, 1993.

[25] I. Talmi, *Simple Models of Complex Nuclei*. Chur: Harwood Academic Publ., 1993.

[26] A. Bohr and B. R. Mottelson, *Nuclear Structure. Volume I. Single-particle motion*. Singapore: World Scientific, 1998.

[27] A. Bohr and B. R. Mottelson, *Nuclear Structure. Volume II. Nuclear Doformations*. Singapore: World Scientific, 1999.

[28] C. A. Bertulani, *Nuclear Physics in a Nutshell*. Princeton: Princeton University Press, 2007.

[29] K. Wildermuth and W. McClure, *Cluster representations of nuclei*. Berlin: Springer, 1966.

[30] Y. Fujiwara, H. Horiuchi, K. Ikeda, M. Kamimura, K. Katō, Y. Suzuki, and E. Uegaki, "Chapter II. Comprehensive Study of Alpha-Nuclei," *Prog. Theor. Phys. Suppl.*, vol. 68, pp. 29–192, 1980.

[31] Yu. M. Shirokov and N. P. Yudin, *Nuclear Physics*. Moscow: 'Mir', 1983.

[32] K. S. Krane, *Introductory Nuclear Physics*. New York: J. Wiley, 1987.

[33] H. Horiuchi, K. Ikeda, and Y. Suzuki, "Chapter III. Molecule-Like Structures in Nuclear System," *Prog. Theor. Phys. Suppl.*, vol. 52, pp. 89–172, 1972.

[34] H. Horiuchi and K. Ikeda, "Cluster Model of the Nucleus," *Cluster Models And Other Topics. Series: International Review of Nuclear Physics, Edited by Y Akaishi, S A Chin and K Ikeda, vol. 4, pp. 1-258*, vol. 4, pp. 1–258, Feb. 1987.

[35] M. Kimura and H. Horiuchi, "^{16}O + ^{16}O molecular nature of the superdeformed band of ^{32}S and the evolution of the molecular structure," *Phys. Rev. C*, vol. 69, pp. 051304–+, May 2004.

[36] J. A. Wheeler, "Molecular Viewpoints in Nuclear Structure," *Phys. Rev.*, vol. 52, pp. 1083–1106, Dec. 1937.

[37] J. A. Wheeler, "On the Mathematical Description of Light Nuclei by the Method of Resonating Group Structure," *Phys. Rev.*, vol. 52, pp. 1107–1122, Dec. 1937.

[38] K. Wildermuth and Y. Tang, *A unified theory of the nucleus*. Braunschweig: Vieweg Verlag, 1977.

[39] L. R. Hafstad and E. Teller, "The Alpha-Particle Model of the Nucleus," *Phys. Rev.*, vol. 54, pp. 681–692, Nov. 1938.

[40] H. Horiuchi, "Chapter III. Kernels of GCM, RGM and OCM and Their Calculation Methods," *Prog. Theor. Phys. Suppl.*, vol. 62, pp. 90–190, 1977.

[41] D. Baye and P.-H. Heenen, "Microscopic R-Matrix theory in a generator coordinate basis (I).

Theory and application to dineutron-dineutron and α-α scattering," *Nucl. Phys. A*, vol. 233, pp. 304–316, Nov. 1974.

[42] D. Baye, P.-H. Heenen, and M. Libert-Heinemann, "Microscopic R-matrix theory in a generator coordinate basis (III). Multi-channel scattering," *Nucl. Phys. A*, vol. 291, pp. 230–240, Nov. 1977.

[43] T. Fliessbach and H. Walliser, "The structure of the resonating group equation," *Nucl. Phys. A*, vol. 377, pp. 84–104, Mar. 1982.

[44] G. F. Filippov and I. P. Okhrimenko, "Use of an oscillator basis for solving continuum problems," *Sov. J. Nucl. Phys.*, vol. **32**, pp. 480–484, 1981.

[45] G. F. Filippov, "On taking into account correct asymptotic behavior in oscillator-basis expansions," *Sov. J. Nucl. Phys.*, vol. **33**, pp. 488–489, 1981.

[46] G. F. Filippov, V. S. Vasilevsky, and L. L. Chopovsky, "Generalized coherent states in nuclear-physics problems," *Sov. J. Part. Nucl.*, vol. **15**, pp. 600–619, 1984.

[47] G. F. Filippov, V. S. Vasilevsky, and L. L. Chopovsky, "Solution of problems in the microscopic theory of the nucleus using the technique of generalized coherent states," *Sov. J. Part. Nucl.*, vol. **16**, pp. 153–177, 1985.

[48] Y. Lashko, G. Filippov, and V. Vasilevsky, "Dynamics of two-cluster systems in phase space," *Nucl. Phys. A*, vol. 941, pp. 121 – 144, 2015.

[49] V. S. Vasilevsky, F. Arickx, J. Broeckhove, and T. P. Kovalenko, "A microscopic three-cluster model with nuclear polarization applied to the resonances of ^7Be and the reaction $^6Li(p,^3He)^4He$," *Nucl. Phys. A*, vol. 824, no. 1-4, pp. 37–57, 2009.

[50] A. V. Nesterov, V. S. Vasilevsky, and T. P. Kovalenko, "Effect of cluster polarization on the spectrum of the ^7Li nucleus and on the reaction $^6Li(n,^3H)^4He$," *Phys. Atom. Nucl.*, vol. 72, pp. 1450–1464, Sept. 2009.

[51] A. V. Nesterov, V. S. Vasilevsky, and T. P. Kovalenko, "Microscopic model of the radiative capture reactions with cluster polarizability. Application to ^7Be and ^7Li.," *Ukr. J. Phys.*, vol. 56, no. 7, pp. 645–653, 2011.

[52] V. S. Vasilevsky, A. V. Nesterov, and T. P. Kovalenko, "Three-cluster model of radiative capture reactions in seven-nucleon systems. Effects of cluster polarization.," *Phys. Atom. Nucl.*, vol. 75, no. 7, pp. 818–831, 2012.

[53] V. S. Vasilevsky, N. Z. Takibayev, and A. D. Duisenbay, "Microscopic description of ^{8}Li and

^{8}B nuclei within three-cluster model," *Ukr. J. Phys.*, vol. 62, no. 6, pp. 461–472, 2017.

[54] Y. A. Lashko, G. F. Filippov, and V. S. Vasilevsky, "Microscopic three-cluster model of ^{10}Be," *Nucl. Phys. A*, vol. 958, pp. 78–100, Feb. 2017.

[55] K. Katō, V. S. Vasilevsky, and N. Z. Takibayev, "Nuclear Cluster Dynamics in Nucleo-Synthesis in Neutron Stars," in *Neutron Stars. Physics, Properties and Dynamics* (N. Z. Takibayev and K. Boshkayev, eds.), ch. 6, pp. 173–226, New-York: Nova Science Publishers, Inc., 2017.

[56] D. R. Tilley, C. M. Cheves, J. L. Godwin, G. M. Hale, H. M. Hofmann, J. H. Kelley, C. G. Sheu, and H. R. Weller, "Energy levels of light nuclei A=5, 6, 7," *Nucl. Phys. A*, vol. 708, pp. 3–163, Sept. 2002.

[57] D. R. Tilley, J. H. Kelley, J. L. Godwin, D. J. Millener, J. E. Purcell, C. G. Sheu, and H. R. Weller, "Energy levels of light nuclei A=8, 9, 10," *Nucl. Phys. A*, vol. 745, pp. 155–362, Dec. 2004.

[58] G. Gamow, "Mass Defect Curve and Nuclear Constitution," *Proc. Royal Soc. London Series A*, vol. 126, pp. 632–644, Mar. 1930.

[59] "Alpha-like four-body correlations and molecular aspects in nuclei," *Prog. Theor. Phys. Suppl.*, vol. **52**, pp. 1–375, 1972.

[60] D. Baye and Y. Salmon, "Generator-coordinate study of elastic ^{16}O + ^{40}Ca scattering," *Nucl. Phys. A*, vol. 331, pp. 264–268, Nov. 1979.

[61] T. Wada, "Study of ^{16}O+^{40}Ca Potential by the Resonating Group Method," *Prog. Theor. Phys.*, vol. 75, pp. 458–460, Feb. 1986.

[62] D. Baye and Y. Salmon, "Generator-coordinate study of elastic ^{40}Ca + ^{40}Ca scattering," *Nucl. Phys. A*, vol. 323, pp. 521–539, July 1979.

[63] A. T. Suzuki and K. Ikeda, "Microscopic Study on Di-Nucleus States of ^{16}O+^{40}Ca and ^{40}Ca+^{40}Ca. I," *Prog. Theor. Phys.*, vol. 69, pp. 113–127, Jan. 1983.

[64] V. S. Vasilevsky, N. Z. Takibayev, and A. D. Duisenbay, "Influence of the cluster polarization on spectrum and reactions in mirror ^{8}Li and ^{8}B nuclei," in *The III International Workshop "Nuclear Physics and Astrophysics", April 14-16*, vol. 3, pp. 24–29, Almaty, Kazakhstan: Phys. Sci. Technol., 2016.

[65] S. Elhatisari, D. Lee, G. Rupak, E. Epelbaum, H. Krebs, T. A. Lähde, T. Luu, and U.-G. Meißner, "Ab initio alpha-alpha scattering," *Nature*, vol. 528, pp. 111–114, Dec. 2015.

[66] F. Ajzenberg-Selove, "Energy levels of light nuclei A = 11-12," *Nucl. Phys. A*, vol. 506, pp. 1–158, Jan. 1990.

[67] P. Navrátil, R. Roth, and S. Quaglioni, "Ab initio many-body calculations of nucleon scattering on ^{4}He, ^{7}Li, ^{7}Be, ^{12}C, and ^{16}O," *Phys. Rev. C*, vol. 82, p. 034609, Sept. 2010.

[68] C. Kurokawa and K. Katō, "Three-alpha resonances in ^{12}C," *Nucl. Phys. A*, vol. 738, pp. 455–458, June 2004.

[69] E. Epelbaum, H. Krebs, D. Lee, and U.-G. Meißner, "Lattice Effective Field Theory Calculations for A=3, 4, 6, 12 Nuclei," *Phys. Rev. Lett.*, vol. 104, p. 142501, Apr. 2010.

[70] V. Vasilevsky, F. Arickx, W. Vanroose, and J. Broeckhove, "Microscopic cluster description of ^{12}C," *Phys. Rev. C*, vol. 85, p. 034318, Mar. 2012.

[71] Y. C. Tang, M. LeMere, and D. R. Thompson, "Resonating group method for nuclear many-body problems," *Phys. Rep.*, vol. **47**, pp. 167–223, 1978.

[72] "Microscopic method for the interactions between complex nuclei," *Prog. Theor. Phys. Suppl.*, vol. **62**, pp. 1–294, 1977.

[73] "Comprehesive study of structure of light nuclei," *Prog. Theor. Phys. Suppl.*, vol. **68**, pp. 1–385, 1980.

[74] M. Kimura and H. Horiuchi, "Introduction of the deformed base AMD and application to the stable and unstable nuclei," *Nucl. Phys. A*, vol. 722, pp. 507–511, July 2003.

[75] H. Feldmeier and T. Neff, "Nuclear Clustering in Fermionic Molecular Dynamics," *ArXiv e-prints*, Dec. 2016.

[76] T. Neff, H. Feldmeier, and R. Roth, "Structure of light nuclei in Fermionic Molecular Dynamics," *Nucl. Phys. A*, vol. 752, pp. 321–324, Apr. 2005.

[77] C. Forssén, E. Caurier, and P. Navrátil, "Charge radii and electromagnetic moments of Li and Be isotopes from the ab initio no-core shell model," *Phys. Rev. C*, vol. 79, p. 021303, Feb. 2009.

[78] B. R. Barrett, P. Navrátil, and J. P. Vary, "Ab initio no core shell model," *Prog. Part. Nucl. Phys.*, vol. 69, pp. 131–181, Mar. 2013.

[79] P. Navrátil, S. Quaglioni, G. Hupin, C. Romero-Redondo, and A. Calci, "Unified ab initio approaches to nuclear structure and reactions," *Phys. Scripta*, vol. 91, p. 053002, May 2016.

[80] M. Abramowitz and A. Stegun, *Handbook of Mathematical Functions.* New-York: Dover Publications, Inc., 1972.

[81] G. F. Filippov, L. L. Chopovsky, and V. S. Vasilevsky, "On ^{7}Li resonances in the $\alpha + t$ channel," *Sov. J. Nucl. Phys.*, vol. **37**, no. 4, pp. 839–846, 1983.

[82] H. A. Yamani and L. Fishman, "J-matrix method: Extensions to arbitrary angular momentum and to Coulomb scattering," *J. Math. Phys.*, vol. **16**, pp. 410–420, 1975.

[83] E. J. Heller and H. A. Yamani, "New L^2 approach to quantum scattering: Theory," *Phys. Rev.*, vol. **A9**, pp. 1201–1208, 1974.

[84] M. H. Macfarlane and J. B. French, "Stripping Reactions and the Structure of Light and Intermediate Nuclei," *Rev. Mod. Phys.*, vol. 32, pp. 567–691, July 1960.

[85] Norman K Glendenning, *Direct nuclear reactions.* Singapore: World Scientific, 1983.

[86] O. F. Nemets, V. G. Neudachin, A. T. Rudchik, Yu. F. Smirnov and Yu. M. Tchuvil'sky, *Nucleon Clusters in Atomic Nuclei and Many-Nucleon Transfer Reactions. (in Russian).* Kiev: 'Naukova Dumka', 1988.

[87] A. Hasegawa and S. Nagata, "Ground state of ^{6}Li," *Prog. Theor. Phys.*, vol. **45**, pp. 1786–1807, 1971.

[88] F. Tanabe, A. Tohsaki, and R. Tamagaki, "$\alpha\alpha$ scattering at intermediate energies," *Prog. Theor. Phys.*, vol. **53**, pp. 677–691, 1975.

[89] V. S. Vasilevsky, F. Arickx, J. Broeckhove, and T. P. Kovalenko, "A microscopic three-cluster model with nuclear polarization applied to the resonances of ^7Be and the reaction $^6Li(p,^3He)^4He$," *Nucl. Phys. A*, vol. 824, pp. 37–57, June 2009.

[90] T. Kajino, T. Matsuse, and A. Arima, "Electromagnetic properties of ^7Li and ^7Be in a cluster model," *Nucl. Phys. A*, vol. 413, pp. 323–352, Jan. 1984.

[91] T. Kajino, G. F. Bertsch, and K. Kubo, "E1 polarizability of ^7Li and astrophysical S factor for $^4He(t,\gamma)^7Li$.," *Phys. Rev. C*, vol. 37, pp. 512–519, 1988.

[92] K. Varga, Y. Suzuki, K. Arai, and Y. Ogawa, "Microscopic description of light unstable nuclei with the stochastic variational method," *Nucl. Phys. A*, vol. 616, pp. 383–393, Feb. 1997.

[93] A. Csótó and R. G. Lovas, "Dynamical microscopic three-cluster description of ^6Li," *Phys. Rev. C*, vol. 46, pp. 576–588, Aug. 1992.

[94] K. Arai, Y. Suzuki, and K. Varga, "Neutron-proton halo structure of the 3.563-MeV 0^+ state in ^6Li," *Phys. Rev. C*, vol. 51, pp. 2488–2493, May 1995.

[95] K. Varga and R. G. Lovas, "Signature of cluster substructure: $\alpha + d$ spectroscopic factor of

^6Li," *Phys. Rev. C*, vol. 43, pp. 1201–1210, Mar. 1991.

[96] S. Saito, "Interaction between Clusters and Pauli Principle," *Prog. Theor. Phys.*, vol. **41**, no. 3, pp. 705–722, 1969.

[97] S. Saito, "Theory of Resonating Group Method and Generator Coordinate Method, and Orthogonality Condition Model," *Prog. Theor. Phys. Suppl.*, vol. **62**, pp. 11–89, 1977.

[98] A. U. Hazi and H. S. Taylor, "Stabilization Method of Calculating Resonance Energies: Model Problem," *Phys. Rev. A*, vol. 1, pp. 1109–1120, Apr. 1970.

[99] R. A. Arndt, L. D. Roper, and R. L. Shotwell, "Analyses of Elastic Proton-Alpha Scattering," *Phys. Rev. C*, vol. 3, pp. 2100–2113, June 1971.

[100] R. A. Arndt, D. D. Long, and L. D. Roper, "Nucleon-alpha elastic scattering analyses (I). Low-energy n-α and p-α analyses," *Nucl. Phys. A*, vol. 209, pp. 429–446, July 1973.

[101] P. Schwandt, T. B. Clegg, and W. Haeberli, "Polarization measurements and phase shifts for $p-^4He$ scattering between 3 and 18 MeV," *Nucl. Phys. A*, vol. 163, pp. 432–448, Mar. 1971.

[102] J. Tirira and F. Bodart, "Alpha-proton elastic scattering analyses up to 4 MeV," *Nuclear Instruments and Methods in Physics Research B*, vol. 74, pp. 496–502, June 1993.

[103] P. Darriulat, G. Igo, H. G. Pugh, and H. D. Holmgren, "Elastic Scattering of Alpha Particles by Helium Between 53 and 120 MeV," *Phys. Rev.*, vol. 137, pp. 315–325, Jan. 1965.

[104] A. D. Bacher, F. G. Resmini, H. E. Conzett, R. de Swiniarski, H. Meiner, and J. Ernst, "Observation of High-Lying Levels in ^{8}Be from α-α Elastic Scattering," *Phys. Rev. Lett.*, vol. 29, pp. 1331–1333, Nov. 1972.

[105] D. R. Thompson, M. LeMere, and Y. C. Tang, "Systematic investigation of scattering problems with the resonating-group method," *Nucl. Phys.*, vol. **A286**, no. 1, pp. 53–66, 1977.

[106] A. B. Volkov, "Equilibrum deformation calculation of the ground state energies of 1p shell nuclei," *Nucl. Phys.*, vol. **74**, pp. 33–58, 1965.

[107] A. S. Davydov, *Quantum Mechanics*. Oxford: Pergamon Press, 1965.

[108] M. Moshinsky, *The Harmonic oscillator in Modern Physics: From Atoms to Quarks*. New-York, London, Paris: Gordon Breach, 1969.

[109] M. Moshinsky and Y. F. Smirnov, *The Harmonic oscillator in Modern Physics*. Amsterdam: Harwood Academic Publ., 1998.

[110] I. V. Kurdyumov, Y. F. Smirnov, K. V. Shitikova, and S. K. E. Samarai, "Translationally

invariant shell model," *Nucl. Phys. A*, vol. 145, pp. 593–612, Apr. 1970.

[111] V. G. Neudachin, Yu. F. Smirnov, *Nucleon associations in light nuclei (in Russian)*. Moscow: 'Nauka', 1969.

[112] Y. I. Nechaev and Y. F. Smirnov, "Solution of the scattering problem in the oscillator representation," *Sov. J. Nucl. Phys.*, vol. **35**, pp. 808–811, 1982.

[113] J. Broeckhove, F. Arickx, P. Hellinckx, V. S. Vasilevsky, and A. V. Nesterov, "The ^5H resonance structure studied with a three-cluster J-matrix model," *J. Phys. G Nucl. Phys.*, vol. 34, pp. 1955–1970, Sept. 2007.

[114] R. G. Newton, *Scattering Theory of Waves and Particles*. New-York: McGraw-Hill, 1966.

[115] P. G. Burke, *Potential scattering in atomic physics*. New York: Plenum Press, 1977.

[116] A. M. Perelomov and Y. B. Zel'dovich, *Quantum Mechanics. Selected Topics*. Singapore, New Jersy, London, Hong Kong: World Scientific, 1998.

[117] V. I. Kukulin, V. M. Krasnopol'sky, and J. Horacek, *Theory of resonances. Principles and applications*. Dordrecht, Boston, London: Kluwer Academic Publishers, 1989.

[118] D. Brink and E. Boeker, "Effective interaction for Hartree-Fock calculations," *Nucl. Phys.*, vol. **A91**, pp. 1–27, 1967.

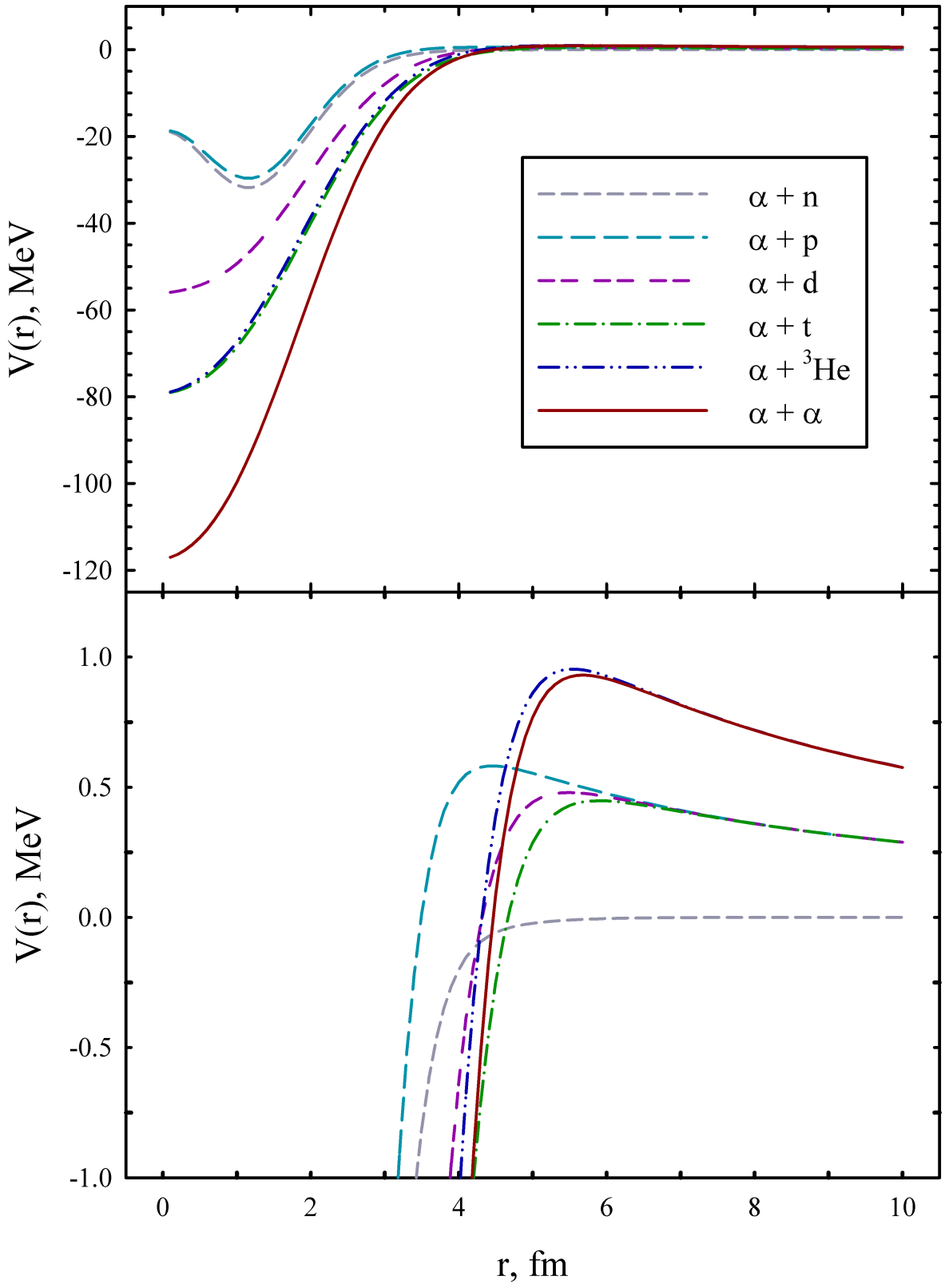

FIG. 22: Folding Potentials as a function of distance between interacting clusters.

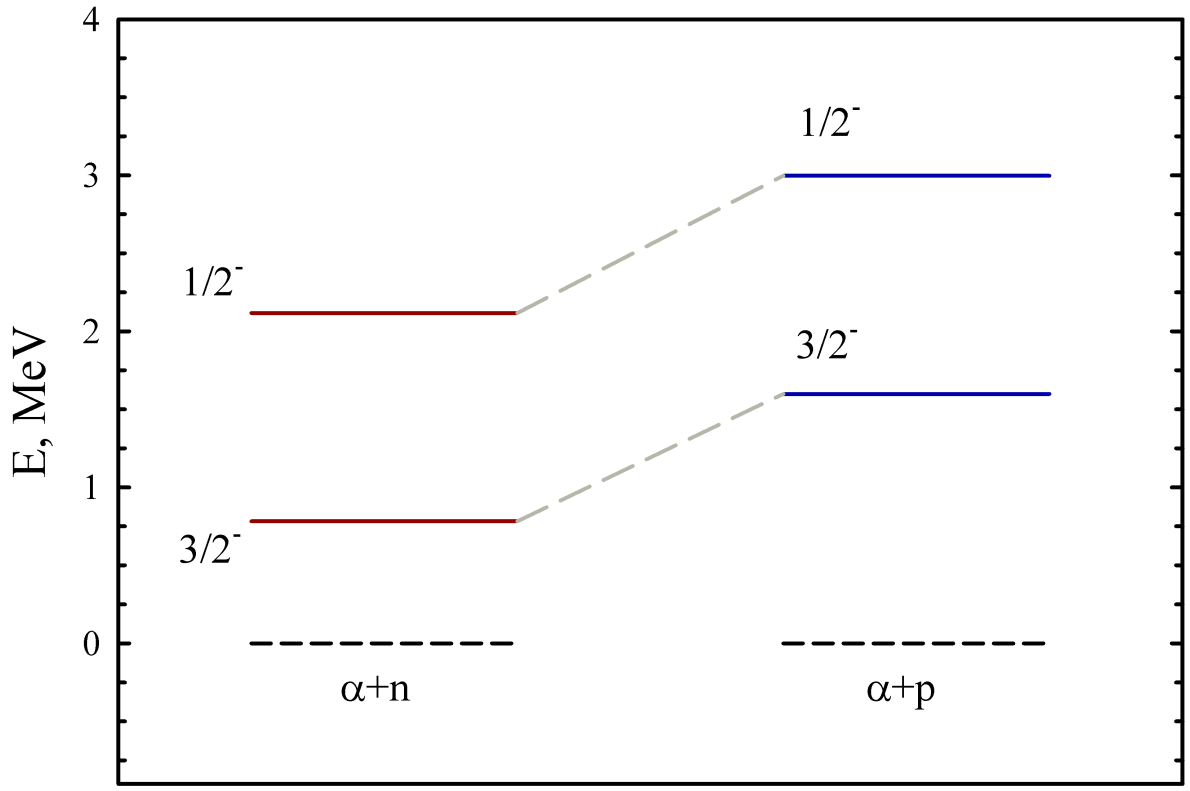

FIG. 23: Spectrum of resonance states in ^{5}He and ^{5}Li.

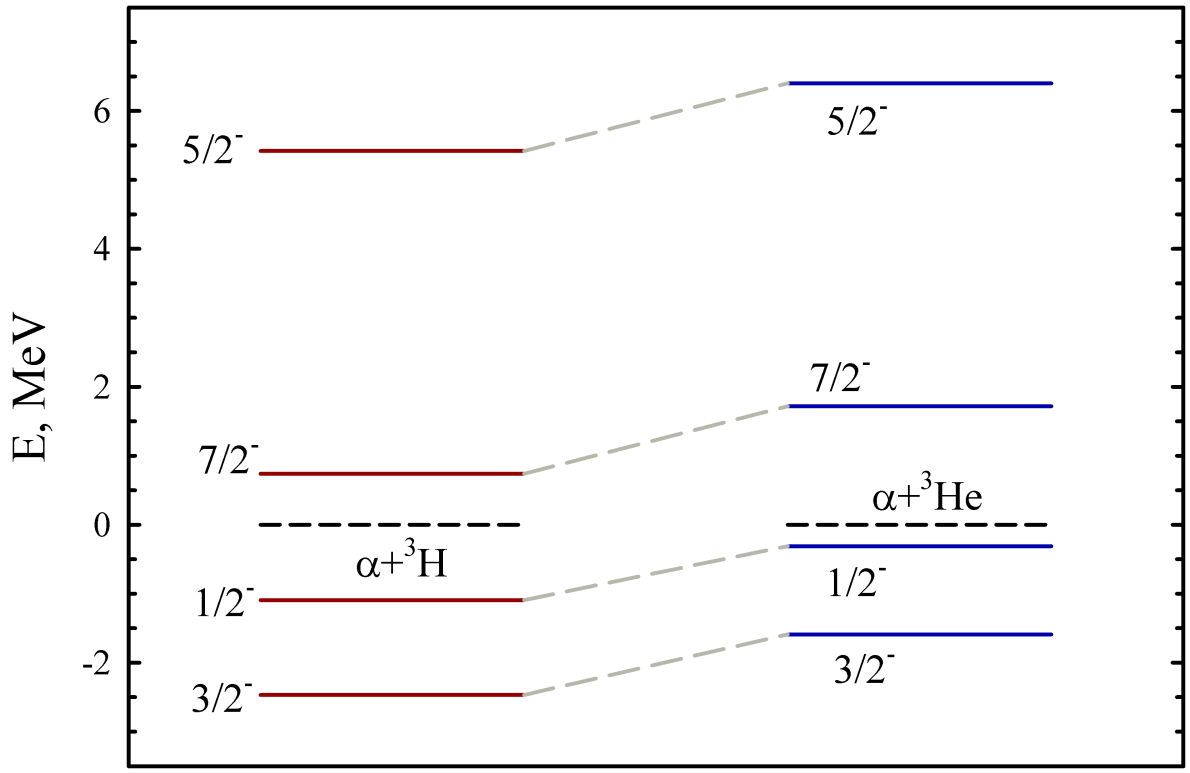

FIG. 24: Effects of the Coulomb interaction of bound and resonance states in mirror nuclei ^{7}Li and ^{7}Be.

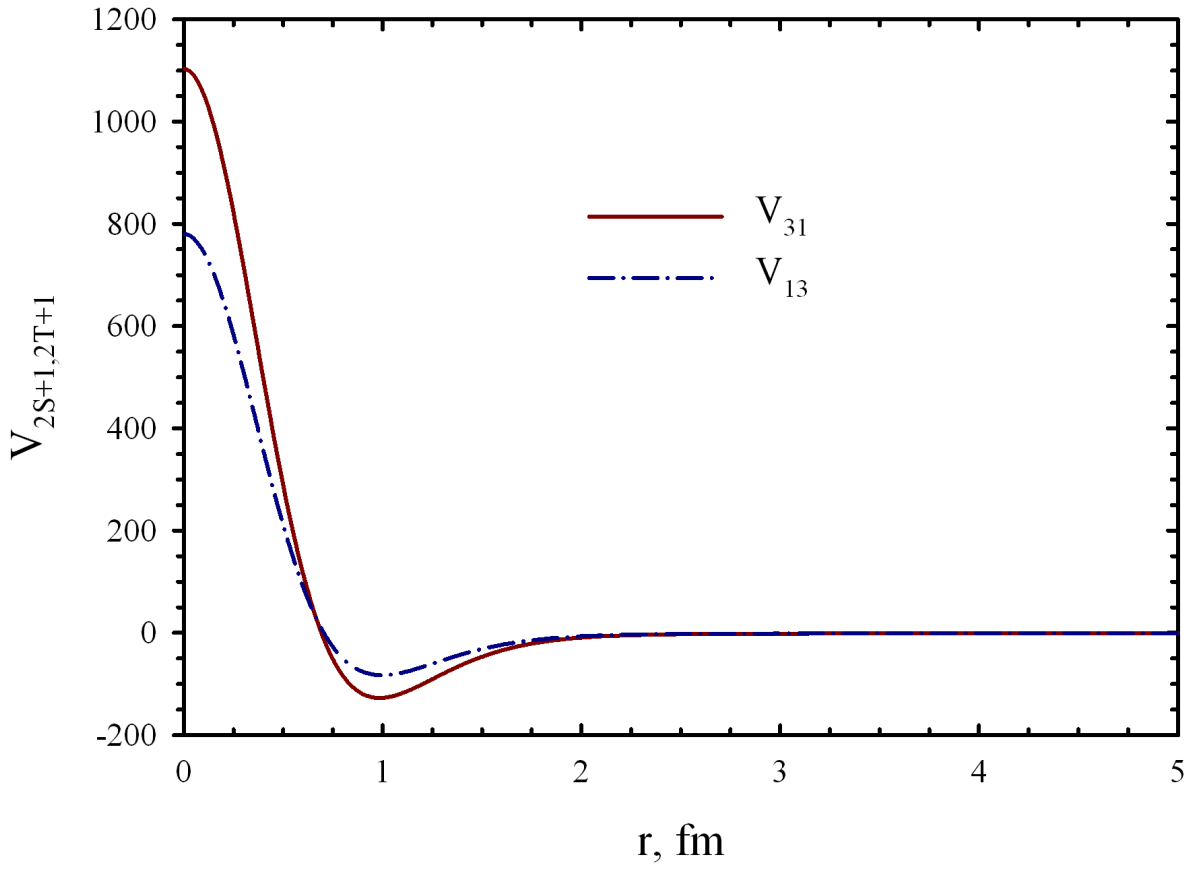

FIG. 25: The even components V_{31} and V_{13} of the modified Hasegawa-Nagata potential as a function of distance between the interacting nucleons.